AEROFOIL AND WING PITCHING MOMENT COEFFICIENT AT ZERO ANGLE OF ATTACK DUE TO DEPLOYMENT OF TRAILING-EDGE DOUBLE-SLOTTED OR TRIPLE-SLOTTED FLAPS AT LOW SPEEDS

1. NOTATION AND UNITS

		SI	*British*
A	aspect ratio, $2s/\bar{c}$		
$(a_1)_0$	basic aerofoil lift-curve slope in incompressible flow	rad^{-1}	rad^{-1}
C_L	lift coefficient; (*lift*)/*qc* for aerofoil, (*lift*)/*qS* for wing		
C_{L0}	C_L at zero angle of attack for aerofoil, based on c		
ΔC_{L0t}	increment in lift coefficient at zero angle of attack due to deployment of trailing-edge double-slotted or triple-slotted flap on aerofoil, based on c (see Item No. 94031)		
$\Delta C'_{L0t}$	increment in lift coefficient at zero angle of attack due to deployment of trailing-edge double-slotted or triple-slotted flap on aerofoil, based on c' (see Item No. 94031)		
$\Delta C'_{L1}, \Delta C'_{L2}$, $\Delta C'_{L3}$	increment in lift coefficient associated with deployment of equivalent first, second, third element of trailing-edge slotted flap on aerofoil with lift-curve slope of 2π, based on c', Figures 4, 5 and 6 (from Item No. 94031)		
C_m	pitching moment coefficient; (*pitching moment*)/qc^2 for aerofoil, (*pitching moment*)/$qS\bar{\bar{c}}$ for wing, referenced to $c/4$ for aerofoil and $\bar{\bar{c}}/4$ for wing, see Sketch 1.1		
C_{m0}	C_m for aerofoil zero lift, based on c^2, see Section 7.1		
C_{m0i}	inviscid value of C_{m0}		
$C_{m\alpha 0}$	pitching moment coefficient at zero angle of attack for aerofoil, based on c^2 and referenced to $c/4$, approximated as C_{m0}, see Section 7.1		
$C_{mw\alpha 0}$	pitching moment coefficient at zero angle of attack for wing, based on $S\bar{\bar{c}}$ and referenced to $\bar{\bar{c}}/4$		
$\Delta C_{mt\alpha 0}$	increment in pitching moment coefficient at zero angle of attack due to deployment of trailing-edge double-slotted or triple-slotted flap on aerofoil, based on c^2 and referenced to $c/4$, see Equation (3.1)		

Issued March 2000 – 34 pages

$\Delta C_{mtw\alpha 0}$	increment in pitching moment coefficient at zero angle of attack due to deployment of trailing-edge double-slotted or triple-slotted flap on wing, based on $S\bar{\bar{c}}$ and referenced to $\bar{\bar{c}}/4$, see Equation (3.11)		
$\Delta C'_{mt\alpha 0}$	increment in pitching moment coefficient at zero angle of attack due to deployment of trailing-edge double-slotted or triple-slotted flap on aerofoil, based on c'^2 and referenced to $c'/4$, see Equation (3.2)		
c	basic (plain) aerofoil chord or wing chord at flap mid-span (*i.e.* chord with high-lift devices undeployed), see Sketches 1.1, 1.2 and 1.3	m	ft
c'	extended aerofoil chord, *i.e.* chord with trailing-edge slotted flap deployed, see Sketches 1.2 and 1.3	m	ft
$\bar{c}$	wing geometric mean chord	m	ft
$\bar{\bar{c}}$	wing aerodynamic mean chord, see Item No. 76003	m	ft
c_{et1}, c_{et2}, c_{et3}	equivalent flap chord of first, second, third element of trailing-edge slotted flap, see Sketch 1.2 for double-slotted flap, Sketch 1.3 for triple-slotted flap	m	ft
c_r	wing root (centre-line) chord, see Sketch 1.1	m	ft
c_{t1}, c_{t2}, c_{t3}	chord of first, second, third element of trailing-edge slotted flap, see Sketch 1.2 for double-slotted flap, Sketch 1.3 for triple-slotted flap	m	ft
Δc_{t1}, Δc_{t2}, Δc_{t3}	increment in c_{t1}, c_{t2}, c_{t3}, see Sketch 1.2 for double-slotted flap, Sketch 1.3 for triple-slotted flap	m	ft
c'_{t1}, c'_{t2}, c'_{t3}	extended chord of first, second, third element of trailing-edge slotted flap, see Sketch 1.2 for double-slotted flap, Sketch 1.3 for triple-slotted flap	m	ft
F	viscous correction factor used in calculation of C_{m0}, see Equation (7.1)		
h_2	centre of incremental lift at zero angle of attack due to trailing-edge slotted flap deployment on aerofoil section expressed as fraction of basic aerofoil chord, measured positive aft from its quarter-chord position		
$h'_{2,1}$, $h'_{2,2}$, $h'_{2,3}$	empirical centre of incremental lift at zero angle of attack associated with deployment of equivalent first, second, third element of trailing-edge slotted flap on aerofoil, expressed as fraction of extended chord, measured positive aft from extended aerofoil quarter-chord position, see Equations (3.5), (3.7) and (3.9)		
$h'_{2,1T}$, $h'_{2,2T}$, $h'_{2,3T}$	theoretical values on which $h'_{2,1}$, $h'_{2,2}$, $h'_{2,3}$ are based, see Equations (3.4), (3.6) and (3.8) and Figure 7		

J_{t1}, J_{t2}, J_{t3}	correlation factor for first, second, third elements of trailing-edge slotted flap, Figures 1, 2 and 3 (from Item No. 94031)		
K	part-span factor; pitching moment coefficient increment due to part-span trailing-edge slotted flaps extending symmetrically from wing centre-line divided by pitching moment coefficient increment due to full-span trailing-edge slotted flaps at same deflection angle, Figure 8		
K_f	flap type correlation factor, (= 1.0)		
$K_{f\Lambda}$	flap type correlation factor for wing sweep, (= 1.0)		
K_i	value of K corresponding to $\eta = \eta_i$, required in Equation (3.11)		
K_o	value of K corresponding to $\eta = \eta_o$, required in Equation (3.11)		
K_Λ	part-span factor dependent on wing sweep effect, Equation (3.14) and Figures 9a to 9f		
$K_{\Lambda i}$	value of K_Λ corresponding to $\eta = \eta_i$, required in Equation (3.11)		
$K_{\Lambda o}$	value of K_Λ corresponding to $\eta = \eta_o$, required in Equation (3.11)		
M	free-stream Mach number		
p	parameter in Equation (3.14) for K_Λ, see Equation (3.15)		
q	free-stream kinetic pressure	N/m^2	lbf/ft^2
R_c	aerofoil Reynolds number, based on free-stream conditions and c		
$R_{\bar{\bar{c}}}$	wing Reynolds number, based on free-stream conditions and $\bar{\bar{c}}$		
S	wing planform area, $2s\bar{c}$	m^2	ft^2
s	wing semi-span, see Sketch 1.1	m	ft
t	maximum thickness of aerofoil	m	ft
x_{ts}	chordwise location of flap-shroud trailing edge, see Sketches 1.2 and 1.3	m	ft
z_{um}	maximum upper-surface ordinate of basic aerofoil, see Sketches 1.2 and 1.3	m	ft
$\delta_{t1}{}^\circ$, $\delta_{t2}{}^\circ$, $\delta_{t3}{}^\circ$	deflection of first, second, third element of trailing-edge slotted flap, positive trailing-edge down, see Sketch 1.2 for double-slotted flap, Sketch 1.3 for triple-slotted flap	deg	deg
η	spanwise distance from wing centre-line as fraction of semi-span		

η_i	value of η at inboard limit of flap, see Sketch 1.1		
η_o	value of η at outboard limit of flap, see Sketch 1.1		
Λ_0	wing leading-edge sweep angle, see Sketch 1.1	deg	deg
$\Lambda_{1/4}$	wing quarter-chord sweep angle, see Sketch 1.1	deg	deg
$\Lambda_{1/2}$	wing half-chord sweep angle	deg	deg
Λ_1	wing trailing-edge sweep angle, see Sketch 1.1	deg	deg
λ	wing taper ratio (tip chord/root chord)		

Subscripts

$(\ )_{expt}$	denotes experimental value
$(\ )_{pred}$	denotes predicted value

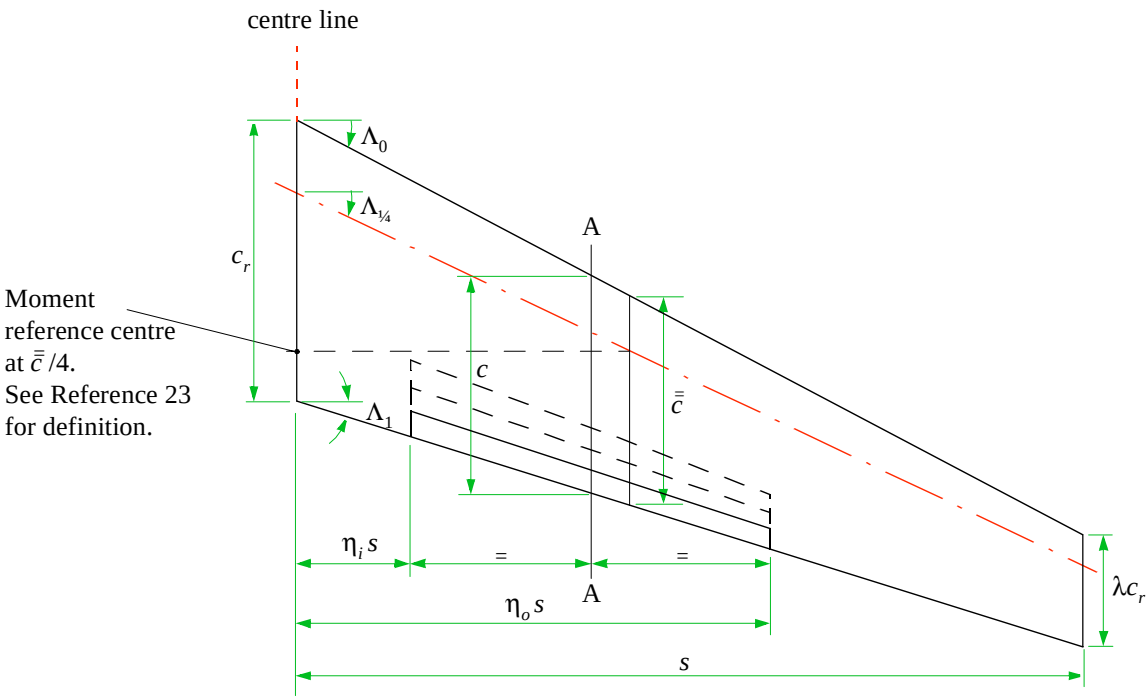

Sketch 1.1 Wing notation (flaps undeployed)

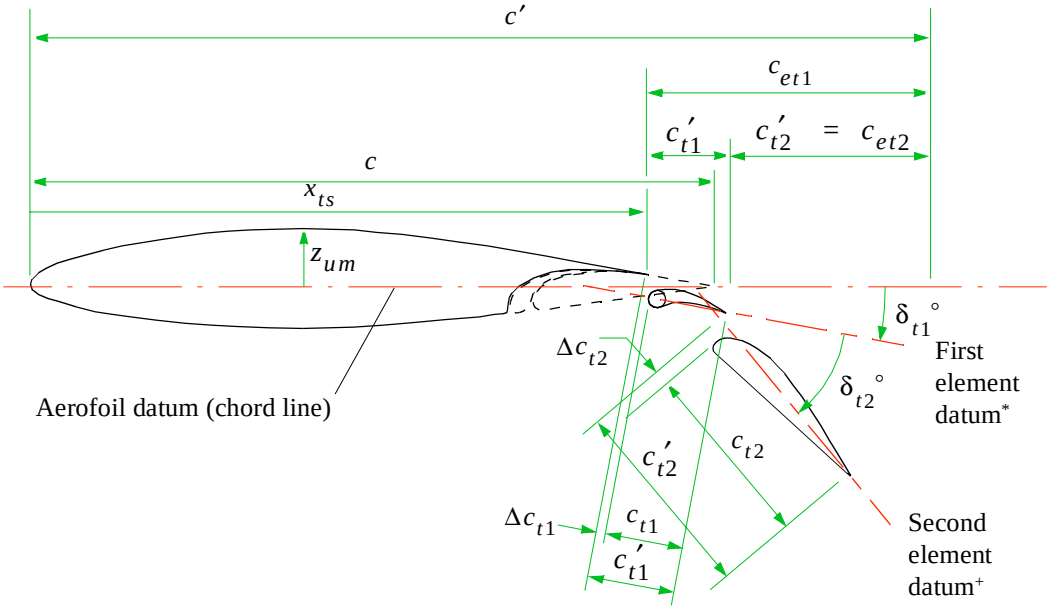

Sketch 1.2 Deployed double-slotted flap notation (at section AA)

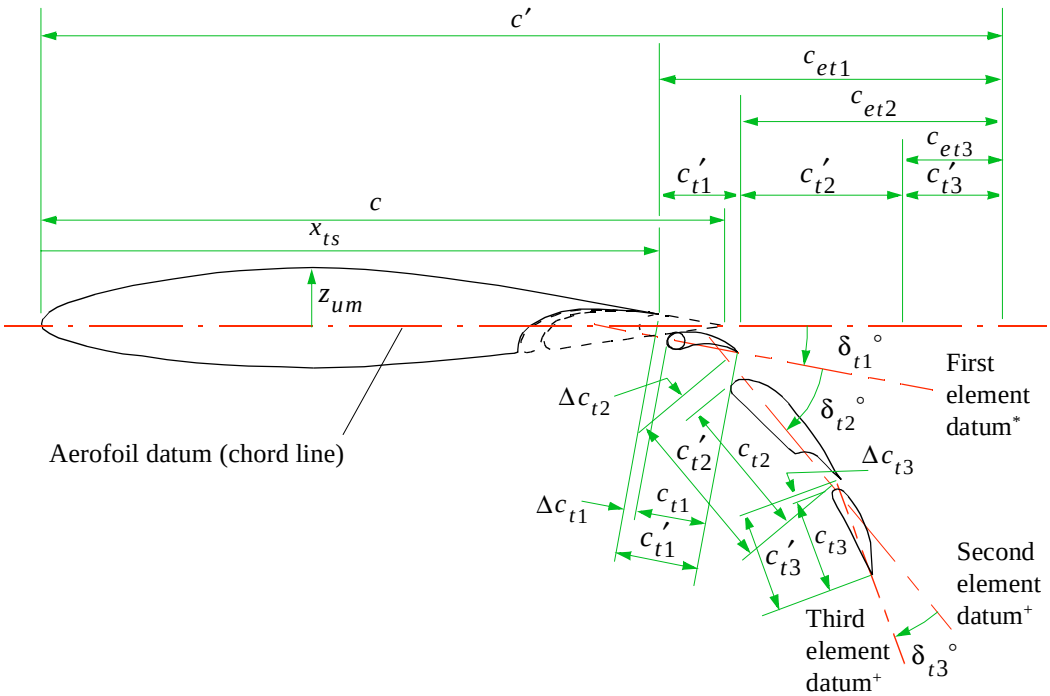

Sketch 1.3 Deployed triple-slotted flap notation (at section AA)

* The deflection of the first flap element, $\delta_{t1}{}^{\circ}$, is the angle between the aerofoil datum line (*i.e.* the aerofoil chord line) and the first element datum line.

The first element datum line is the chord line of the element, defined as the line passing through the centre of the leading-edge radius and the trailing edge.

\+ The deflection of the second flap element, $\delta_{t2}{}^{\circ}$, is the angle between the first and second element datum lines.

The deflection of the third flap element, $\delta_{t3}{}^{\circ}$, is the angle between the second and third element datum lines.

In contrast to the definition of the datum line of the first flap element, the datum lines of the second and third flap elements are the rotated aerofoil datum line considered to be fixed in each element.

2. INTRODUCTION

This Item provides a method to obtain the increment in pitching moment coefficient at zero angle of attack due to deployment of trailing-edge double-slotted or triple-slotted flaps at low speeds, either on an aerofoil or on a wing.

For aerofoils the method predicts the centre of lift position, $h_{2,1}$, $h_{2,2}$ and $h_{2,3}$, due to deployment of each element of a double-slotted or triple-slotted flap, based on the thin-aerofoil theory of Derivation 19 and modified to obtain correlation with the experimental data of Derivations 3, 5, 6, 7, 8, 10, 13, 17 and 18. Each centre of lift position is combined with the increment in aerofoil lift coefficient for the corresponding element calculated from Item No. 94031 (Derivation 2) to estimate the total pitching moment coefficient increment. When applied to a multi-element flap, thin-aerofoil theory represents each element as an 'equivalent' single-element flap (of chord c_{et1} *etc.*, see Sketches 1.2 and 1.3), and their moment contributions are summed.

For wings with full-span flaps, factors, dependent on planform geometry, are applied to the pitching moment coefficient increment on a section that is representative of the wing, to allow for three-dimensional effects. Derivations 20 and 21 are used as the basis for these factors, with some adjustment to the simple theoretical assumptions. For wings with part-span flaps, additional factors are introduced that are dependent on taper ratio, aspect ratio, sweep and spanwise extent of the flap.

Section 3 describes the prediction method and Section 4 discusses Mach number and Reynolds number effects. The applicability and accuracy of the method are addressed in Section 5. The Derivation and References are given in Section 6. Section 7 provides worked examples illustrating the use of the Item for an aerofoil and a wing.

3. PREDICTION METHOD

The method for aerofoils requires the use of Item No. 94031 to determine the lift increment characteristics of the aerofoil/flap combination from which to derive the pitching moment coefficient increment.

For wings, the *streamwise* section, flap geometries and angles at the mid-span of the flap panel are taken to be representative of the wing/flap system, see Sketches 1.1, 1.2 and 1.3. The method again requires the use of Item No. 94031 to determine the lift increment characteristics of the representative section/flap combination from which to derive the section pitching moment coefficient increment. By this means the effects of spanwise variation are averaged out. Empirical corrections allow for the effects of wing planform geometry and the spanwise extent of the flaps.

3.1 Aerofoil Pitching Moment Coefficient Increment $\Delta C_{mt\alpha 0}$

The increment in pitching moment coefficient at zero angle of attack, due to deployment of a double-slotted or triple-slotted flap on an aerofoil, is obtained from

$$\Delta C_{mt\alpha 0} = \Delta C'_{mt\alpha 0}(c'/c)^2 - \Delta C'_{L0t}\,(c'/c)(c'/c-1)/4 - C_{L0}(c'/c-1)/4 + C_{m\alpha 0}(c'/c-1)\ . \qquad (3.1)$$

Here, $\Delta C'_{mt\alpha 0}$ is the increment in pitching moment coefficient at zero angle of attack due to deployment of a double-slotted or triple-slotted flap on an aerofoil, based on the extended chord, and is evaluated as

$$\Delta C'_{mt\alpha 0} = -[J_{t1}\Delta C'_{L1}h'_{2,1} + J_{t2}\Delta C'_{L2}h'_{2,2} + J_{t3}\Delta C'_{L3}h'_{2,3}](a_1)_0/2\pi\ , \qquad (3.2)$$

and $\Delta C'_{L0t}$ is the increment in lift coefficient at zero angle of attack due to deployment of a double-slotted or triple-slotted flap on an aerofoil, based on the extended chord, and is evaluated as

$$\Delta C'_{L0t} = [J_{t1}\Delta C'_{L1} + J_{t2}\Delta C'_{L2} + J_{t3}\Delta C'_{L3}](a_1)_0/2\pi, \tag{3.3}$$

where J_{t1}, J_{t2}, J_{t3}, $\Delta C'_{L1}$, $\Delta C'_{L2}$ and $\Delta C'_{L3}$ are given in Figures 1 to 6 respectively, reproduced from Item No. 94031. The basic aerofoil lift-curve slope, $(a_1)_0$, in incompressible flow, may be obtained from Item No. Wings 01.01.05 (Derivation 1) and the flap deflection angles, $\delta_{t1}{}^\circ$, $\delta_{t2}{}^\circ$ and $\delta_{t3}{}^\circ$, are in degrees. The formulae for J_{t1}, J_{t2} and J_{t3} are included on Figures 1 to 3.

The centre of the lift increment due to the first flap element at zero angle of attack, $h'_{2,1}$, is expressed as a fraction of the extended chord and measured positive aft from the quarter-chord point of the extended aerofoil chord. It is derived empirically from its theoretical value in Derivation 19 for a hinged plate on a thin aerofoil and adjusted to allow for chord extension by replacing c_{t1}/c with c_{et1}/c' to give

$$h'_{2,1T} = \frac{0.25[1-(2c_{et1}/c'-1)^2]^{1/2}[1-(2c_{et1}/c'-1)]}{\left\{\pi - \cos^{-1}(2c_{et1}/c'-1) + [1-(2c_{et1}/c'-1)^2]^{1/2}\right\}}. \tag{3.4}$$

An incremental adjustment to obtain correlation with experimental data gives

$$h'_{2,1} = h'_{2,1T} - 4(z_{um}/c)^{1.5}(x_{ts}/c - 1), \tag{3.5}$$

where x_{ts}/c is the chordwise location of the flap-shroud trailing edge as a fraction of the basic aerofoil chord and z_{um}/c is the ratio of the maximum upper-surface ordinate to the aerofoil chord, see Sketches 1.2 and 1.3.

Following the model of Equation (3.4), the theoretically derived centre of the lift increment due to the second flap element at zero angle of attack is

$$h'_{2,2T} = \frac{0.25[1-(2c_{et2}/c'-1)^2]^{1/2}[1-(2c_{et2}/c'-1)]}{\left\{\pi - \cos^{-1}(2c_{et2}/c'-1) + [1-(2c_{et2}/c'-1)^2]^{1/2}\right\}}. \tag{3.6}$$

No adjustment is required to obtain correlation with experimental data, so that

$$h'_{2,2} = h'_{2,2T}. \tag{3.7}$$

Similarly, for the third flap element

$$h'_{2,3T} = \frac{0.25[1-(2c_{et3}/c'-1)^2]^{1/2}[1-(2c_{et3}/c'-1)]}{\left\{\pi - \cos^{-1}(2c_{et3}/c'-1) + [1-(2c_{et3}/c'-1)^2]^{1/2}\right\}}, \tag{3.8}$$

where again no adjustment is required to obtain correlation with experimental data, so that

$$h'_{2,3} = h'_{2,3T} \,. \tag{3.9}$$

Values of $h'_{2,1T}$, $h'_{2,2T}$ and $h'_{2,3T}$, determined respectively from Equations (3.4), (3.6) and (3.8), are given in Figure 7 as a function of c_{et1}/c', c_{et2}/c' and c_{et3}/c'.

The final terms in Equation (3.1) involving C_{L0} and $C_{m\alpha 0}$, the lift and pitching moment coefficients at zero angle of attack for the basic aerofoil, provide an approximation to the effect of extension of the aerofoil without flap angular rotation. (Note that the term involving $C_{m\alpha 0}$ is always small compared to the first two terms in Equation (3.1) and it is sufficient to use C_{m0} in place of $C_{m\alpha 0}$, see Section 7.1). The method must not be used to obtain pitching moment increments due to extension without rotation of at least one of the slotted flap elements, since the values due to extension alone are critically dependent on detailed geometry not accounted for in the method. As shown in Table 5.1, the minimum validated combined flap deflection angle for double-slotted flaps is $|\delta_{t1}°| + \delta_{t2}° = 20°$.

The centre of incremental lift at zero angle of attack due to flap deployment, expressed as a fraction of the *basic* aerofoil chord and referred to its quarter-chord position, is obtained from

$$h_2 = \frac{-\Delta C_{mt\alpha 0}}{\Delta C'_{L0t}\,(c'/c)} \,. \tag{3.10}$$

3.2 Wing Pitching Moment Coefficient Increment $\Delta C_{mtw\alpha 0}$

For a wing at zero angle of attack the increment in pitching moment coefficient due to slotted flap deployment is

$$\Delta C_{mtw\alpha 0} = K_f(K_o - K_i)\Delta C_{mt\alpha 0} + K_{f\Lambda}(K_{\Lambda o} - K_{\Lambda i})(A/2)\Delta C'_{L0t}\,(c'/c)\tan\Lambda_{1/4}\,, \tag{3.11}$$

where A is the wing aspect ratio, $\Lambda_{1/4}$ is the wing quarter-chord sweep angle, and $\Delta C'_{L0t}$ and $\Delta C_{mt\alpha 0}$ are now calculated from Equations (3.3) and (3.1), respectively, for the representative streamwise section of the wing, taken at flap mid-span.

The part-span factors K_i and K_o are obtained from Figure 8 as functions of wing taper ratio and the inboard and outboard limits of the flap, $\eta = \eta_i$ and η_o, respectively.

The flap-type correlation factors for double-slotted and triple-slotted flaps have been derived from the data of Derivations 4, 9, 11, 12 and 14 to be

$$K_f = 1.0 \tag{3.12}$$

and

$$K_{f\Lambda} = 1.0\,. \tag{3.13}$$

The part-span wing-sweep factors, $K_{\Lambda i}$ and $K_{\Lambda o}$, are obtained for slotted flaps from Figures 9a to 9f as functions of the extended chord ratio, c'/c, and the inboard and outboard limits of the flap, $\eta = \eta_i$ and η_o respectively, for a range of values of wing taper ratio. Note that for all cases with a full-span flap or an unswept quarter-chord line the second term in Equation (3.11) has a value of zero.

The data for K_Λ given in Figures 9a to 9f for $\lambda = 0$, 0.1, 0.2, 0.4, 0.6 and 1 were obtained from Derivation 20 for extended flaps in the form

$$K_\Lambda = \frac{-3(1+\lambda)}{4(1+\lambda+\lambda^2)}\left\{\left[0.5\eta^2 - 0.333(1-\lambda)\eta^3\right]\left[(c'/c)(1-p)+p\right] - \left[0.5 - 0.333(1-\lambda)\right]p\right\}, \quad (3.14)$$

where λ is the wing taper ratio

and $$p = \frac{(c'/c)[\eta - 0.5(1-\lambda)\eta^2]}{0.5(1+\lambda) - [\eta - 0.5(1-\lambda)\eta^2](1-c'/c)}. \quad (3.15)$$

4. EFFECTS OF MACH NUMBER AND REYNOLDS NUMBER

4.1 Mach Number Effects

High local Mach numbers will occur at low free-stream Mach number as a result of high angle deployment of slotted flaps. Significant Mach number effects will occur at free-stream Mach numbers greater than about 0.2, at large values of $\delta_{t1}°$, $\delta_{t2}°$ and $\delta_{t3}°$ and at progressively smaller values of these angles as Mach number is increased. None of the data considered for this Item was for a Mach number greater than 0.2.

4.2 Reynolds Number Effects

Values of $\Delta C_{mt\alpha 0}$ and $\Delta C_{mtw\alpha 0}$ are derived with an aerofoil lift-curve slope, $(a_1)_0$ (obtained from Item No. Wings 01.01.05), which is dependent on Reynolds number. For the data used in the derivation of this Item no additional effect of Reynolds number on $\Delta C_{mt\alpha 0}$ or $\Delta C_{mtw\alpha 0}$ was found over the ranges of Reynolds number shown in Tables 5.1 and 5.2.

5. APPLICABILITY AND ACCURACY

5.1 Applicability

5.1.1 Aerofoils

The method given in this Item for estimating the position of the centre of the lift increment and the increment in pitching moment coefficient at zero angle of attack due to deployment of a trailing-edge double-slotted or triple-slotted flap applies only to aerofoils without the deployment of a leading-edge device.

Table 5.1 summarises the parameter ranges covered by the experimental data, obtained from Derivations 3, 5, 6, 7, 8, 10, 13, 17 and 18, correlated by Equations (3.5), (3.7) and (3.9).

TABLE 5.1 Parameter ranges for test data for trailing-edge double-slotted and triple-slotted flaps on aerofoils used in the method of Section 3.1

Parameter	*Range*	
	Double-slotted flaps	*Triple-slotted flaps*
t/c	0.08 to 0.15	0.15
z_{um}/c	0.05 to 0.095	0.086
c_{t1}/c	0.056 to 0.227	0.131
c_{t2}/c	0.23 to 0.26	0.244
c_{t3}/c	Not applicable	0.161
c'/c	1.02 to 1.23	1.34
$\Delta c_{t1}/c$	–0.115 to 0.015	–0.02
$\Delta c_{t2}/c$	–0.084 to 0	–0.02
$\Delta c_{t3}/c$	Not applicable	–0.007
x_{ts}/c	0.715 to 0.854	0.850
$\delta_{t1}{}^\circ$	–10° to 35°	14°
$\delta_{t2}{}^\circ$	10° to 45°	41°
$\delta_{t3}{}^\circ$	Not applicable	20°
$\lvert\delta_{t1}{}^\circ\rvert + \delta_{t2}{}^\circ$	20° to 80°	55° (= 14° + 41°)
$\delta_{t1}{}^\circ + \delta_{t2}{}^\circ + \delta_{t3}{}^\circ$	Not applicable	75° (= 14° + 41° + 20°)
$R_c \times 10^{-6}$	1.8 to 8.0	1.8
M	≤ 0.2	0.12

5.1.2 Wings

The method given in this Item for estimating the increment in pitching moment coefficient, at zero angle of attack, due to deployment of a trailing-edge double-slotted flap on a wing, has been shown to be applicable to straight-tapered wings covering a wide range of planform parameters. Table 5.2 summarises the parameter ranges covered by the experimental data that were obtained from Derivations 4, 9, 11, 12, 14, 15 and 16 and used in the development of the method.

For a wing where c_{t1}/c, c_{t2}/c or c_{t3}/c is not constant, the flap should be divided into several spanwise portions, a calculation made separately for each portion, using its mid-span geometry, and the results summed to provide a total value of $\Delta C_{mtw\alpha 0}$. The number of portions required will depend on how rapidly the ratio c_{t1}/c, c_{t2}/c or c_{t3}/c varies across the span.

No wings with cranked leading or trailing edges or curved tips were included in the analysis. It is suggested that for such wings the planform parameters λ and $\Lambda_{1/4}$ be calculated for the equivalent straight-tapered planform as defined in Item No. 76003 (Reference 23). Care should be taken with the definition of c_{t1}/c, c_{t2}/c and c_{t3}/c and the user of the final result should be aware of the non-validated use of the method for such wings.

The method has only been validated for wings without leading-edge devices. In the case of triple-slotted flaps the validation is for aerofoils but not for wings. However, in view of the satisfactory correlation obtained for both double-slotted and triple-slotted flaps on aerofoils and for double-slotted flaps on wings there is no reason to expect poorer correlation for triple-slotted flaps on wings.

TABLE 5.2 Parameter ranges for test data for trailing-edge double-slotted flaps on wings used in the method of Section 3.2

Parameter	*Range*		
A	3.5	to	10.0
$A\tan\Lambda_0$	0.4	to	6.6
$A\tan\Lambda_{1/2}$	–0.4	to	5.5
Λ_0	0	to	49°
Λ_1	–8°	to	38°
λ	0.3	to	1.0
t/c	0.07	to	0.18
z_{um}/c	0.035	to	0.106
c_{t1}/c	0.06	to	0.16
c_{t2}/c	0.19	to	0.4
$(c_{t1}+c_{t2})/c$	0.25	to	0.55
c_{t1}/c_{t2}	0.27	to	0.56
c'/c	1.09	to	1.3
$\Delta c_{t1}/c$	–0.025	to	0.01
$\Delta c_{t2}/c$	–0.08	to	0.016
x_{ts}/c	0.71	to	0.86
$\delta_{t1}{}^\circ$	5°	to	45°
$\delta_{t2}{}^\circ$	19°	to	40°
$\delta_{t1}{}^\circ+\delta_{t2}{}^\circ$	24°	to	67°
η_i	0	to	0.16
η_o	0.36	to	1.0
$R\frac{=}{c}\times10^{-6}$	0.5	to	10.0
M		$\leq$	0.2

5.2 Accuracy

5.2.1 Aerofoils

Sketch 5.1 shows the comparison between predicted and experimental values of h_2, the centre of the lift increment due to the deployment of double-slotted or triple-slotted flaps on an aerofoil, for data from Derivations 3, 5, 6, 7, 8, 10, 13, 17 and 18; the rms error is 0.0154 and 90% of the data are correlated to within ± 0.02. Sketch 5.2 shows the corresponding comparison between predicted and experimental values of pitching moment coefficient increments, where the rms error is 0.035 and 90% of the data are correlated to within ± 0.04.

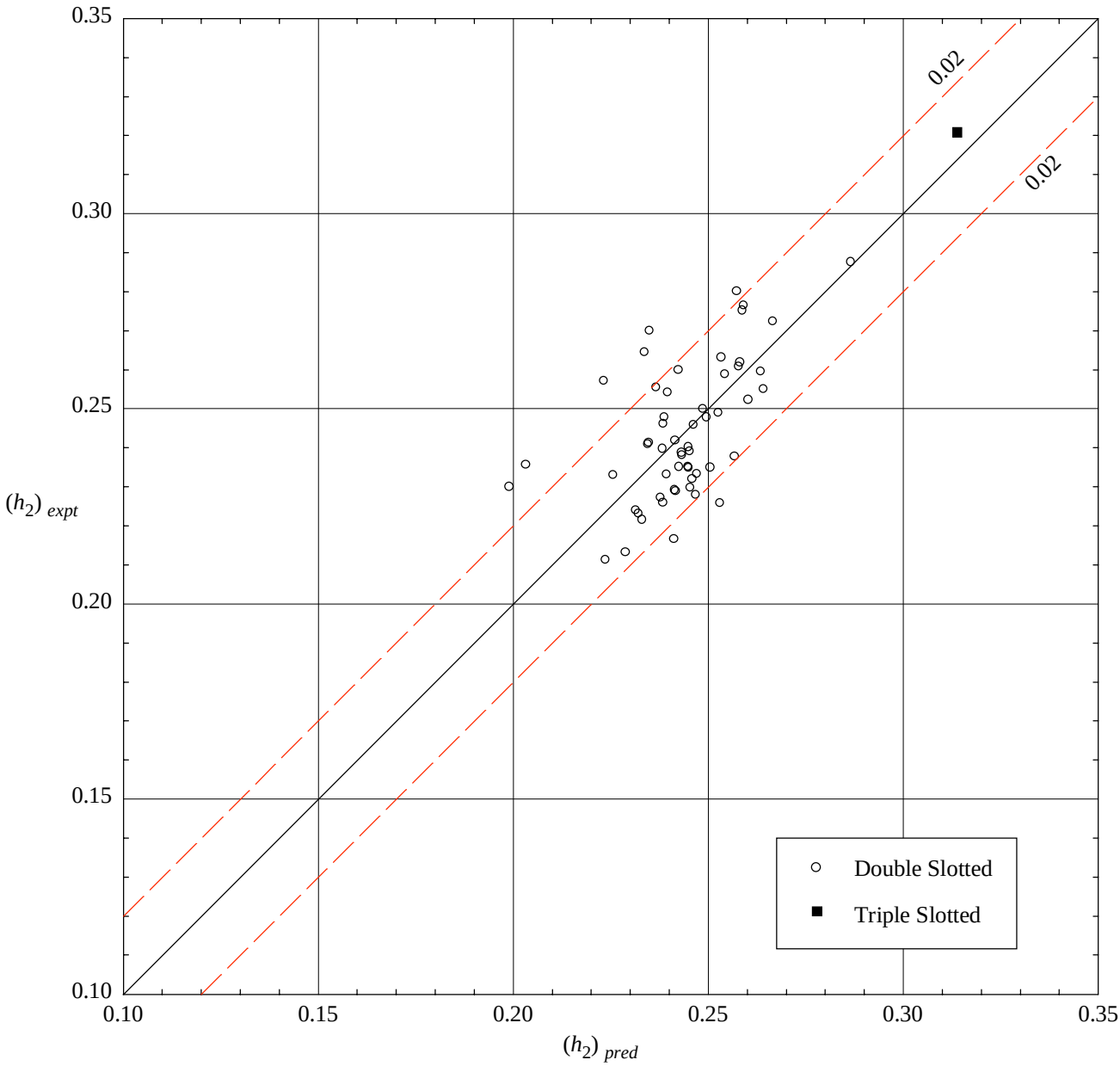

Sketch 5.1 Comparison of predicted and experimental values of h_2 for deployment of double-slotted and triple-slotted flaps

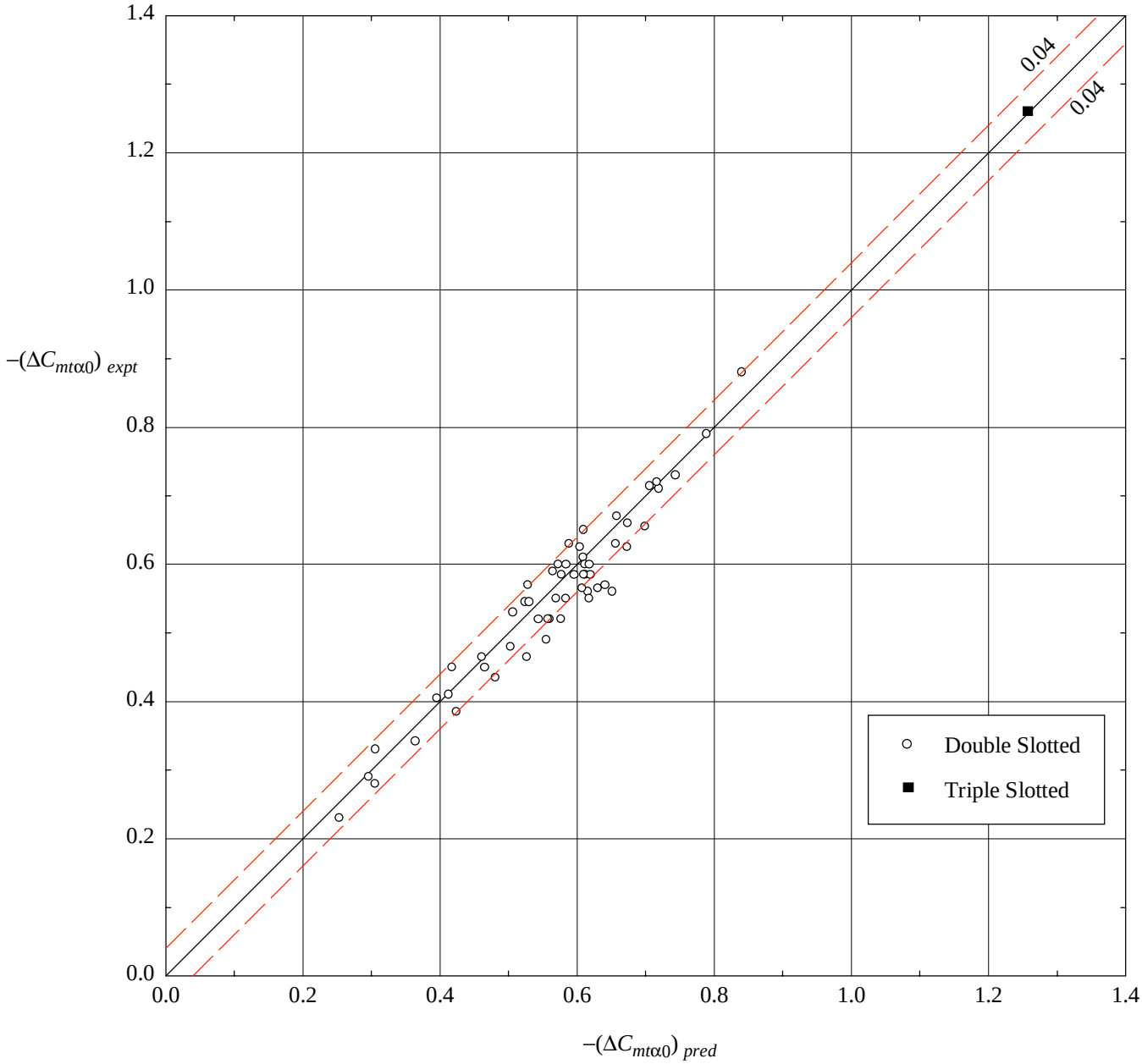

Sketch 5.2 Comparison of predicted and experimental values of $\Delta C_{mt\alpha 0}$ for deployment of double-slotted and triple-slotted flaps on aerofoils

5.2.2 Wings

The comparison between predicted and experimental values of the pitching moment coefficient increment, $\Delta C_{mtw\alpha 0}$, due to deployment of both full-span and part-span double-slotted flaps is shown on Sketch 5.3 for unswept wings and on Sketch 5.4 for swept wings, for data from Derivations 4, 9, 11, 12, 14, 15 and 16. In the two sketches 86% of the data points are within ±0.04 and the rms error is 0.0265.

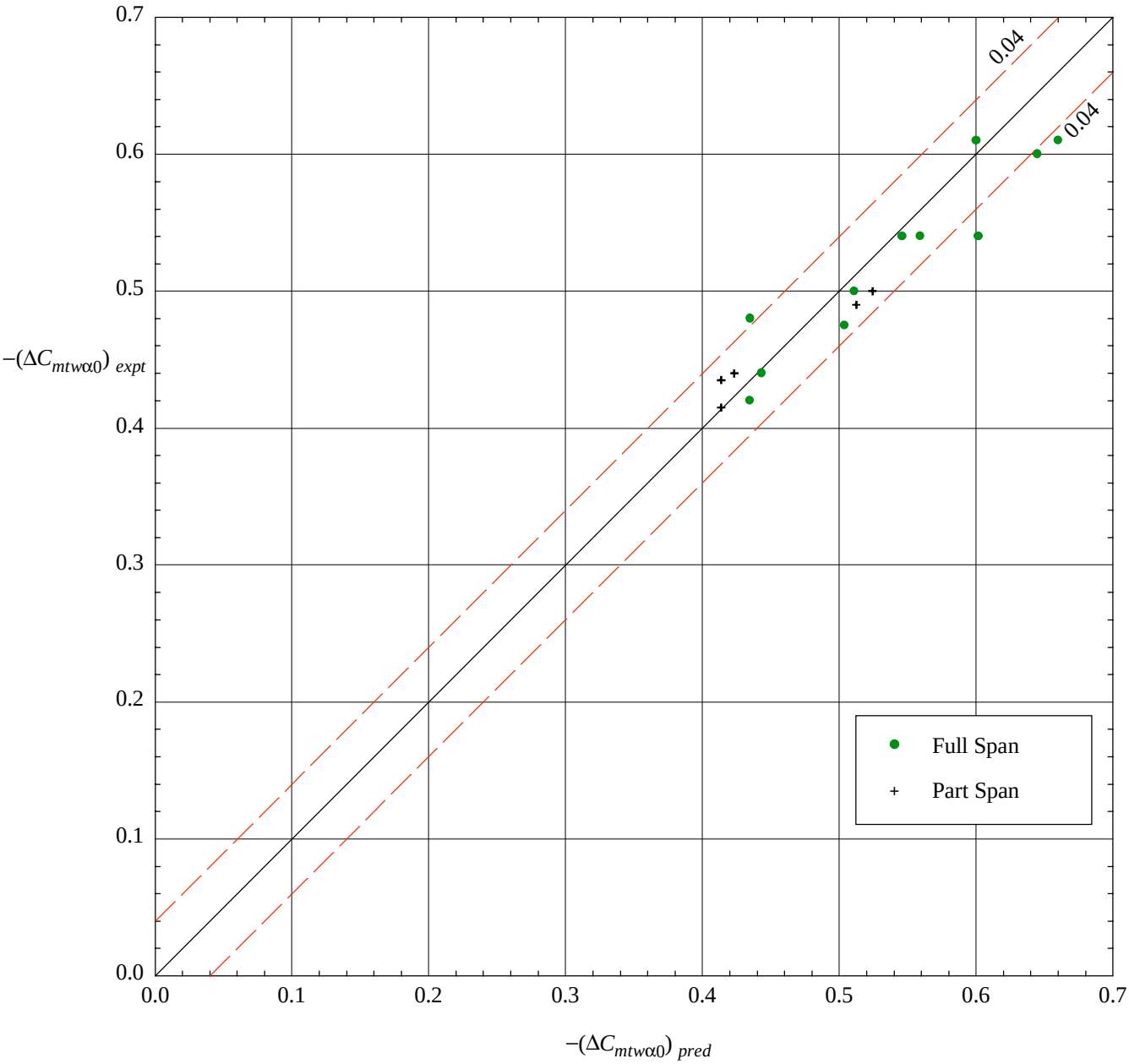

Sketch 5.3 Comparison of predicted and experimental values of $\Delta C_{mtw\alpha 0}$ for deployment of double-slotted flaps on unswept wings

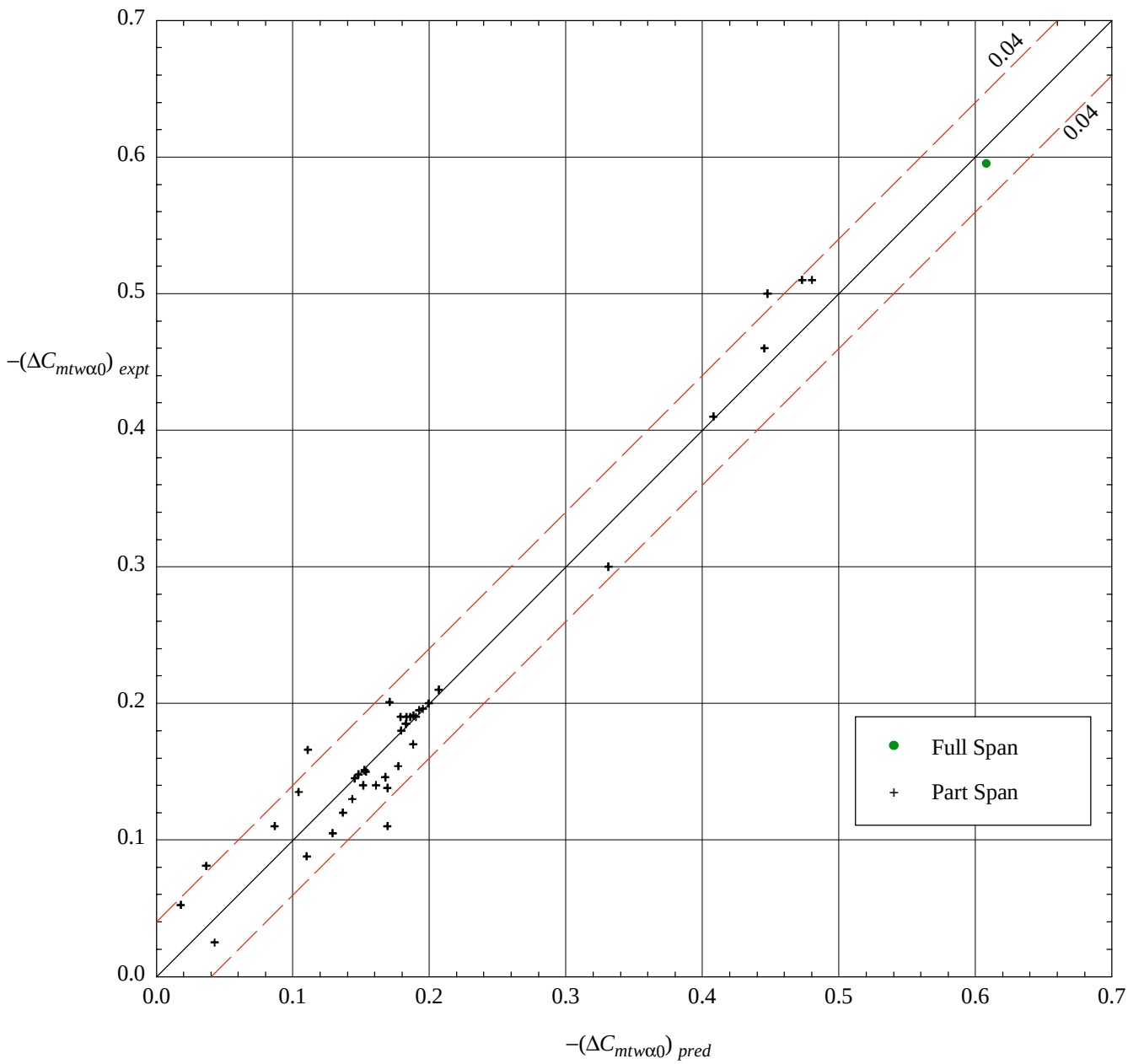

Sketch 5.4 Comparison of predicted and experimental values of $\Delta C_{mtw\alpha 0}$ for deployment of double-slotted flaps on swept wings

6. DERIVATION AND REFERENCES

6.1 Derivation

The Derivation lists selected sources of information that have been used in the preparation of this Item.

6.1.1 ESDU Data Items

1.	ESDU	Slope of lift curve for two-dimensional flow. ESDU International, Item No. Wings 01.01.05, 1955.
2.	ESDU	Increments in aerofoil lift coefficient at zero angle of attack and in maximum lift coefficient due to deployment of a double-slotted or triple-slotted trailing-edge flap, with or without a leading-edge high-lift device, at low speeds. ESDU International, Item No. 94031, 1995.

6.1.2 Wind-tunnel test reports

3.	HARRIS, T.A. RECANT, I.G.	Wind-tunnel investigation of NACA 23012, 23021 and 23030 airfoils equipped with 40-percent-chord double-slotted flaps. NACA Report 723, 1941.
4.	BLACKBURN AIRCRAFT	Wind tunnel tests on moderately large chord flaps with single and multiple slots. Blackburn Aircraft Limited, Report W.T. 85/42, 1943.
5.	BOGDONOFF, S.M.	Wind-tunnel investigation of a low-drag airfoil section with a double-slotted flap. NACA ACR 3I20 (TIL 494), 1943.
6.	BRASLOW, A.L. LOFTIN, L.K.	Two-dimensional wind-tunnel investigation of an approximately 14-percent-thick NACA 66-series-type airfoil section with a double-slotted flap. NACA tech. Note 1110, 1946.
7.	CAHILL, J.F.	Two-dimensional wind-tunnel investigation of four types of high-lift flap on a NACA 65-210 airfoil section. NACA tech. Note 1191, 1947.
8.	CAHILL, J.F. RACISZ, S.F.	Wind-tunnel investigation of seven thin aerofoil sections to determine optimum double-slotted-flap configurations. NACA tech. Note 1545, 1947.
9.	SIVELLS, J.C. SPOONER, S.H.	Investigation in the Langley 19-foot pressure tunnel of two wings of NACA 65-210 and 64-210 airfoil sections with various type flaps. NACA Report 942, 1947.
10.	VISCONTI, F.	Wind-tunnel investigation of air loads over a double-slotted flap on the NACA 65(216)-215 a=0.8 airfoil section. NACA RM L7A30 (TIL 1355), 1947.

11. KOVEN, W. GRAHAM, R.R. — Wind-tunnel investigation of high lift and stall control devices on a 37° sweptback wing of aspect ratio 6. NACA RM L8D29 (TIL 1907), 1948.

12. SALMI, R.J. — Effects of leading-edge devices and trailing-edge flaps on longitudinal characteristics of two 47.7° sweptback wings of aspect ratio 5.1 and 6 at a Reynolds number of 6.0×10^6. NACA RM L50F20 (TIL 2446), 1950.

13. KELLY, J.A. HAYTER, N.-L.F. — Lift and pitching moment at low speeds of the NACA 64A010 airfoil section equipped with various combinations of a leading-edge slat, leading-edge flap, split flap and double-slotted flap. NACA tech. Note 3007, 1953.

14. NAESETH, R.L. — Low speed aerodynamic characteristics of a 45° sweptback wing with double-slotted flaps. NACA RM L56A10 (TIL 5052), 1956.

15. NAESETH, R.L. — Effect of a fuselage on the low-speed longitudinal aerodynamic characteristics of a 45° sweptback wing with double-slotted flaps. NACA RM L56G02 (TIL 5247), 1956.

16. NAESETH, R.L. DAVENPORT, E.E. — Investigation of double-slotted flaps on a swept wing transport model. NASA tech. Note D-103, 1959.

17. LJUNGSTROM, B.L.G. — 2-D wind-tunnel experiments with double and triple-slotted flaps. Aeronaut. Res. Inst., Sweden. FFA AU-993, 1973.

18. LJUNGSTROM, B.L.G. — Wind-tunnel high-lift optimisation of a multiple element airfoil. Aeronaut. Res. Inst., Sweden. FFA AU-778, 1976.

6.1.3 Theory

19. GLAUERT, H. — Theoretical relationships for an aerofoil with hinged flap. ARC R&M 1095, 1927.

20. DENT, M.M. CURTIS, M.F. — A method of estimating the effect of flaps on pitching moment and lift on tailless aircraft. RAE Report No. Aero 1861, 1943.

21. YOUNG, A.D. — The aerodynamic characteristics of flaps. ARC R&M 2622 (RAE Report No. Aero 2185), 1947.

6.1.4 References

The References are sources of information supplementary to that used in the derivation of this Item.

22. ESDU — Aerodynamic characteristics of aerofoils in compressible inviscid airflow at subcritical Mach numbers. ESDU International, Item No. 72024, 1972.

23. ESDU Geometrical properties of cranked and straight tapered wing planforms.
ESDU International, Item No. 76003, 1976.

24. ESDU Wing pitching moment at zero lift at subcritical Mach numbers.
ESDU International, Item No. 87001, 1987.

25. ESDU Slope of aerofoil lift curve for subsonic two-dimensional flow.
ESDU International, Item No. 97020, 1997.

26. ESDU Aerofoil incidence for zero lift in subsonic two-dimensional flow.
ESDU International, Item No. 98011, 1998.

7. EXAMPLES

7.1 Example 1: Pitching Moment Increment due to a Trailing-edge Double-slotted Flap on an Aerofoil

Estimate the increment in pitching moment coefficient at zero angle of attack due to the deployment of a double-slotted trailing-edge flap installed on a modified NACA 65_2-215 section as shown in Sketch 7.1. The modifications produced a linear profile rearwards from 75% chord and 65% chord on the upper and lower surfaces respectively.

The required geometrical parameters are as follows.

Aerofoil	*Flap*		
$z_{um}/c = 0.086$	$x_{ts}/c = 0.85$		
	$c_{t1}/c = 0.12$	$\delta_{t1}° = 20°$	$\Delta c_{t1}/c = 0.02$
	$c_{t2}/c = 0.24$	$\delta_{t2}° = 25°$	$\Delta c_{t2}/c = -0.01$

The flow conditions are $M = 0.2$ and $R_c = 4.5 \times 10^6$, both of which are within the ranges of Table 5.1.

The inviscid value, C_{m0i}, of the pitching moment coefficient for aerofoil zero lift, which may be calculated by the method in Item No. 72024 (Reference 22), is taken as -0.031 for $M = 0.2$.

The angle of attack for zero lift, which may be calculated by the method in Item No. 98011 (Reference 26), is taken as $-1.004°$ for the given flow conditions.

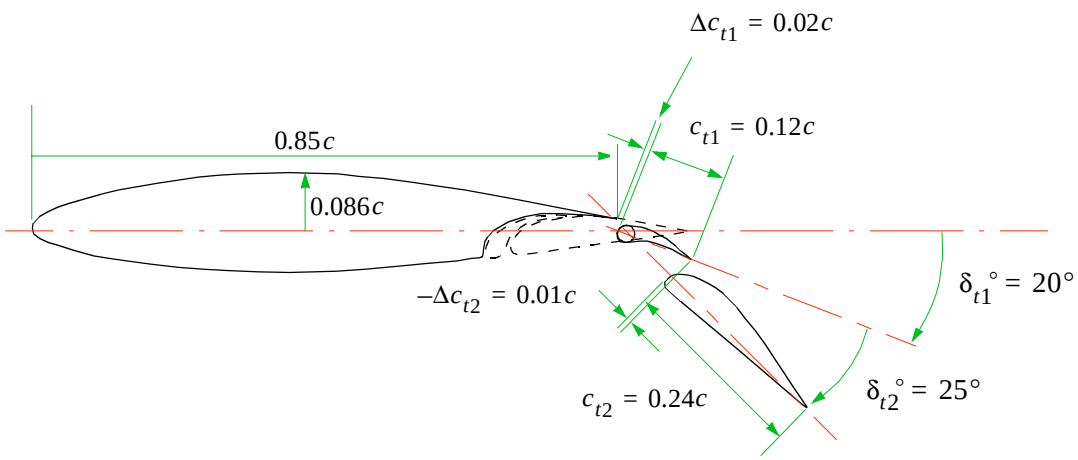

Sketch 7.1 Flap Geometry

(1) Obtain C_{L0} and $C_{m\alpha 0}$

For the modified NACA 65_2–215 section, from Item No. Wings 01.01.05 (Derivation 1) for boundary-layer transition at the leading edge

$$(a_1)_0 = 5.62 \text{ rad}^{-1} .$$

(Although a more accurate estimate of the lift-curve slope is available by the method of Item No. 97020 (Reference 25), the value from Item No. Wings 01.01.05 is used because the method of that Item was employed in the original correlation of flap lift coefficient increments.)

The angle of attack for zero lift is given as –1.004°

so that $$C_{L0} = -5.62 \times (-1.004 / 57.3) = 0.10 .$$

As remarked in Section 3.1, the term in Equation (3.1) involving $C_{m\alpha 0}$ is always small compared with the first two terms so it is acceptable to assume that for the basic aerofoil the pitching moment at zero angle of attack is equal to the pitching moment at zero lift, *i.e.* $C_{m\alpha 0} = C_{m0}$. This assumption is exact for all cases in which the aerodynamic centre is at the quarter-chord point.

The inviscid value of C_{m0} at $M = 0.2$ is given as $C_{m0i} = -0.031$. Figure 1 of Item No. 87001 (Reference 24) provides a viscous correction factor *F*, which can be approximated by the equation

$$F = 1 - 0.29\left[\sin\left(\frac{-C_{m0i}}{0.29}\frac{\pi}{2}\right)\right]^{0.7} \text{, where the angle is measured in radians,} \qquad (7.1)$$

so that $$F = 1 - 0.29\left[\sin\left(\frac{0.031}{0.29}\frac{\pi}{2}\right)\right]^{0.7}$$

$$= 0.917 ,$$

and hence, through the assumption noted above,

$$C_{m\alpha 0} = C_{m0} = FC_{m0i} = 0.917 \times (-0.031)$$
$$= -0.028 .$$

(2) Obtain c'/c, c_{et1}/c' and c_{et2}/c'

From the definitions of Sketch 1.2, the dimensions of Sketch 7.1 give

$$c'_{t1}/c = c_{t1}/c + \Delta c_{t1}/c$$
$$= 0.12 + 0.02$$
$$= 0.14 ,$$

$$c'_{t2}/c = c_{t2}/c + \Delta c_{t2}/c$$
$$= 0.24 - 0.01$$
$$= 0.23 ,$$

and the aerofoil extended chord ratio, c'/c is

$$c'/c = x_{ts}/c + c'_{t1}/c + c'_{t2}/c$$
$$= 0.85 + 0.14 + 0.23$$
$$= 1.22 .$$

The equivalent chords of the first and second flap elements are

$$c_{et1}/c = c'_{t1}/c + c'_{t2}/c$$
$$= 0.14 + 0.23$$
$$= 0.37$$

and

$$c_{et2}/c = c'_{t2}/c$$
$$= 0.23 ,$$

so that

$$c_{et1}/c' = (c_{et1}/c) / (c'/c)$$
$$= 0.37 / 1.22$$
$$= 0.303$$

and

$$c_{et2}/c' = (c_{et2}/c) / (c'/c)$$
$$= 0.23 / 1.22$$
$$= 0.189 .$$

(3) Determine $\Delta C'_{L0t}$

From Equation (3.3), for a double-slotted flap

$$\Delta C'_{L0t} = [J_{t1}\Delta C'_{L1} + J_{t2}\Delta C'_{L2}](a_1)_0/2\pi \qquad (7.2)$$

in which, from

Figure 1 with $\delta_{t1}{}^{\circ} = 20^{\circ}$,

$$J_{t1} = 1.154$$

and, from Figure 4 with $\delta_{t1}{}^{\circ} = 20^{\circ}$ and $c_{et1}/c' = 0.303$,

$$\Delta C'_{L1} = 1.068 \ .$$

Also,

Figure 2 with $\delta_{t1}{}^{\circ} = 20^{\circ}$ gives

$$J_{t2} = 1.40$$

(note that J_{t2} is a function $\delta_{t1}{}^{\circ}$, not $\delta_{t2}{}^{\circ}$)

and Figure 5 with $\delta_{t2}{}^{\circ} = 25^{\circ}$ and $c_{et2}/c' = 0.189$ gives

$$\Delta C'_{L2} = 0.712 \ .$$

Therefore, from Equation (7.2),

$$\begin{aligned}\Delta C'_{L0t} &= (1.154 \times 1.068 + 1.40 \times 0.712) \times 5.62/(2\pi) \\ &= (1.232 + 0.997) \times 5.62/(2\pi) \\ &= 1.994 \ .\end{aligned}$$

(4) Determine $h'_{2,1}$

From Equation (3.4), with the inverse cosine evaluated in radians,

$$h'_{2,1T} = \frac{0.25[1-(2c_{et1}/c'-1)^2]^{1/2}[1-(2c_{et1}/c'-1)]}{\left\{\pi - \cos^{-1}(2c_{et1}/c'-1) + [1-(2c_{et1}/c'-1)^2]^{1/2}\right\}}$$

$$= \frac{0.25[1-(2\times 0.303-1)^2]^{1/2}[1-(2\times 0.303-1)]}{\left\{\pi - \cos^{-1}(2\times 0.303-1) + [1-(2\times 0.303-1)^2]^{1/2}\right\}}$$

$$= 0.1536 \ ,$$

Alternatively, the value of $h'_{2,1T}$ could be read from Figure 7.

From Equation (3.5)

$$h'_{2,1} = h'_{2,1T} - 4(z_{um}/c)^{1.5}(x_{ts}/c-1)$$

$$= 0.1536 - 4\times(0.086)^{1.5}\times(0.85-1)$$

$$= 0.1687 \ .$$

(5) Determine $h'_{2,2}$

From Equation (3.6), with the inverse cosine evaluated in radians,

$$h'_{2,2T} = \frac{0.25[1-(2c_{et2}/c'-1)^2]^{1/2}[1-(2c_{et2}/c'-1)]}{\left\{\pi - \cos^{-1}(2c_{et2}/c'-1) + [1-(2c_{et2}/c'-1)^2]^{1/2}\right\}}$$

$$= \frac{0.25[1-(2\times 0.189-1)^2]^{1/2}[1-(2\times 0.189-1)]}{\left\{\pi - \cos^{-1}(2\times 0.189-1) + [1-(2\times 0.189-1)^2]^{1/2}\right\}}$$

$$= 0.1887.$$

Alternatively, as before the value could be read from Figure 7.

From Equation (3.7)

$$h'_{2,2} = h'_{2,2T}$$

$$= 0.1887 \ .$$

(6) Determine $\Delta C'_{mt\alpha 0}$

From Equation (3.2), for a double-slotted flap,

$$\begin{aligned}
\Delta C'_{mt\alpha 0} &= -[J_{t1}\Delta C'_{L1}h'_{2,1} + J_{t2}\Delta C'_{L2}h'_{2,2}]\,(a_1)_0/2\pi \\
&= -[1.154 \times 1.068 \times 0.1687 + 1.400 \times 0.712 \times 0.1887] \times 5.62/(2\pi) \\
&= -[0.2068 + 0.1881] \times 0.8945 \\
&= -0.3532\ .
\end{aligned}$$

(7) Determine $\Delta C_{mt\alpha 0}$

From Equation (3.1)

$$\begin{aligned}
\Delta C_{mt\alpha 0} &= -\Delta C'_{mt\alpha 0}\,(c'/c)^2 - \Delta C'_{L0t}\,(c'/c)(c'/c - 1)/4 \\
&\qquad - C_{L0}(c'/c - 1)/4 + C_{m\alpha 0}(c'/c - 1) \\
&= -0.3532 \times 1.22^2 - 1.994 \times 1.22 \times (1.22 - 1)/4 \\
&\qquad - 0.10 \times (1.22 - 1)/4 - 0.028 \times (1.22 - 1) \\
&= -0.5257 - 0.1338 - 0.0055 - 0.0062 \\
&= -0.6712 \\
&\approx \mathbf{-0.671}\ .
\end{aligned}$$

The centre of incremental lift expressed as a fraction of the basic aerofoil chord and referred to its quarter-chord position is obtained by evaluation of Equation (3.10) from which

$$\begin{aligned}
h_2 &= \frac{-\Delta C_{mt\alpha 0}}{\Delta C'_{L0t}(c'/c)} \\
&= \frac{0.6712}{1.994 \times 1.22} \\
&= 0.276.
\end{aligned}$$

7.2 Example 2: Pitching Moment Increment due to a Trailing-edge Double-slotted Flap on a Wing

Estimate the increment in pitching moment coefficient at zero angle of attack for a Reynolds number $R_{\bar{\bar{c}}} = 4.5 \times 10^6$ and a free-stream Mach number $M = 0.2$ for a wing with a part-span double-slotted trailing-edge flap as shown in Sketch 7.2. The wing has the planform parameter values

$$A = 8, \Lambda_{1/4} = 25° \text{ and } \lambda = 0.4$$

and across the whole span the streamwise section is the modified NACA 65_2–215 profile which was used in Example 1.

The flap has the same streamwise geometrical parameters as those used in Example 1 and extends from the wing centre-line to 60% of the wing semi-span.

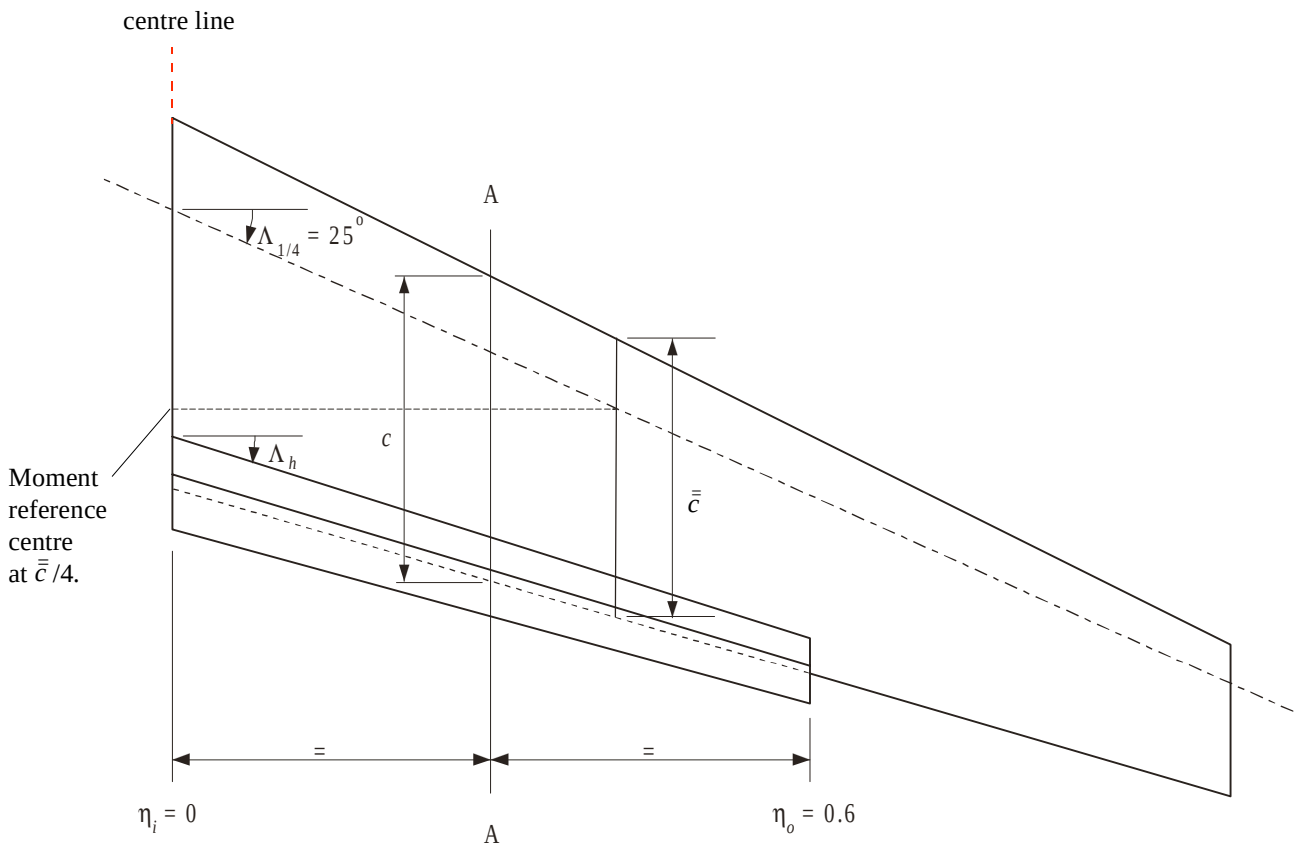

Sketch 7.2 Wing planform with deployed flap

The derived sweep angles $\Lambda_0 = 27.5°$ and $\Lambda_1 = 17°$ (see Item No. 76003, Reference 23), the parameter $A \tan \Lambda_0 = 4.16$, the Mach number and the Reynolds number all lie within the ranges shown on Table 5.2.

Determine $\Delta C_{mtw\alpha 0}$

In addition to the incremental coefficients

$$\Delta C_{mt\alpha 0} = -0.671 .$$

and

$$\Delta C'_{L0t} = 1.994$$

for the aerofoil section from Example 1, various factors are needed to determine $\Delta C_{mtw\alpha 0}$ from Equation (3.11).

The flap type correlation factors K_f and $K_{f\Lambda}$ are given by Equations (3.12) and (3.13) as

$$K_f = K_{f\Lambda} = 1.0 .$$

From Figure 8 for $\eta_i = 0$

$$K_i = 0$$

and for $\eta_o = 0.6$ and $\lambda = 0.4$

$$K_o = 0.788 .$$

From Figure 9d for $\lambda = 0.4$, $c'/c = 1.22$ and $\eta_i = 0$

$$K_{\Lambda i} = 0$$

and for $\eta_o = 0.6$

$$K_{\Lambda o} = 0.0526 .$$

Therefore, from Equation (3.11)

$$\begin{aligned}
\Delta C_{mtw\alpha 0} &= K_f(K_o - K_i)\Delta C_{mt\alpha 0} + K_{f\Lambda}(K_{\Lambda o} - K_{\Lambda i})(A/2)\Delta C'_{L0t}\,(c'/c)\tan\Lambda_{1/4} \\
&= 1.0 \times (0.788 - 0) \times (-0.671) + 1.0 \times (0.0526 - 0) \times (8/2) \times 1.994 \times 1.22 \times \tan 25^\circ \\
&= -0.5287 + 0.2387 \\
&= \mathbf{-0.290} .
\end{aligned}$$

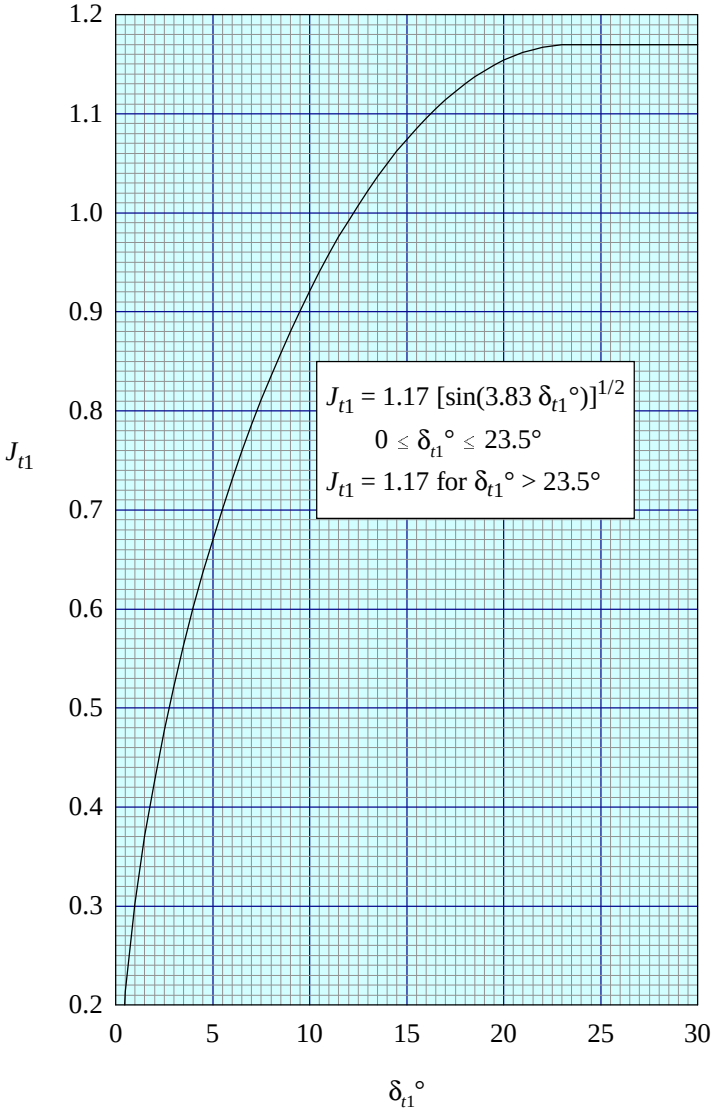

FIGURE 1 CORRELATION FACTOR FOR FIRST ELEMENT OF SLOTTED FLAP

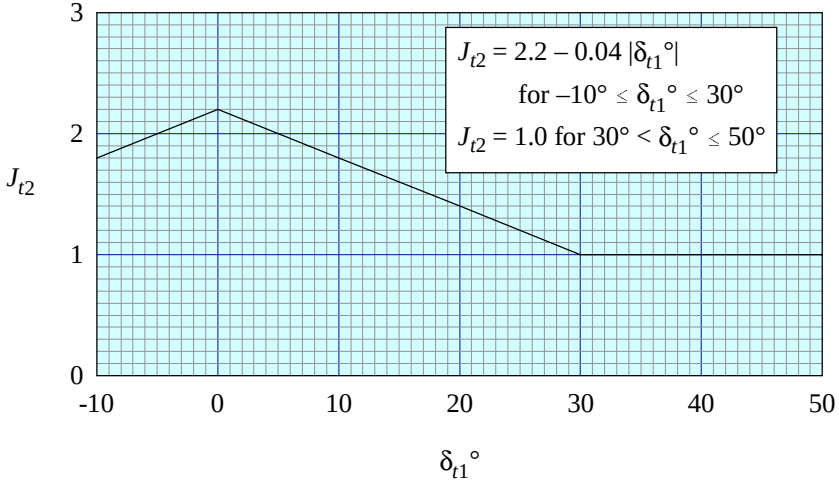

FIGURE 2 CORRELATION FACTOR FOR SECOND ELEMENT OF SLOTTED FLAP

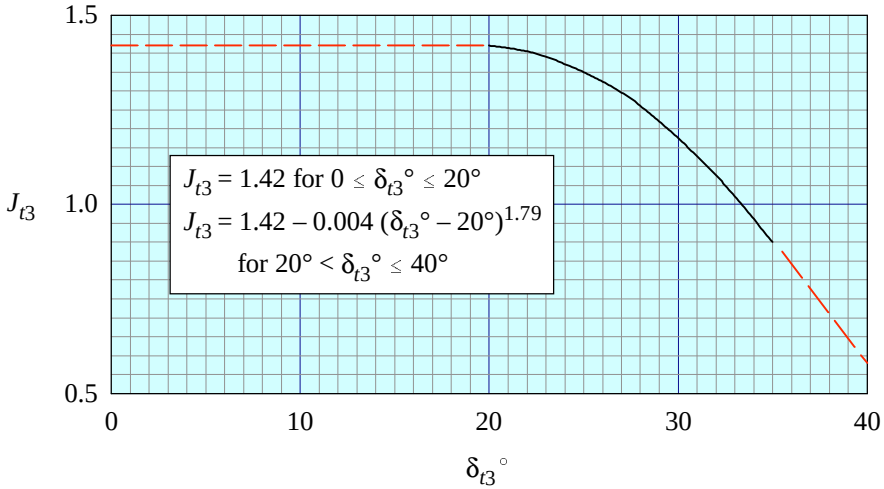

FIGURE 3 CORRELATION FACTOR FOR THIRD ELEMENT OF SLOTTED FLAP

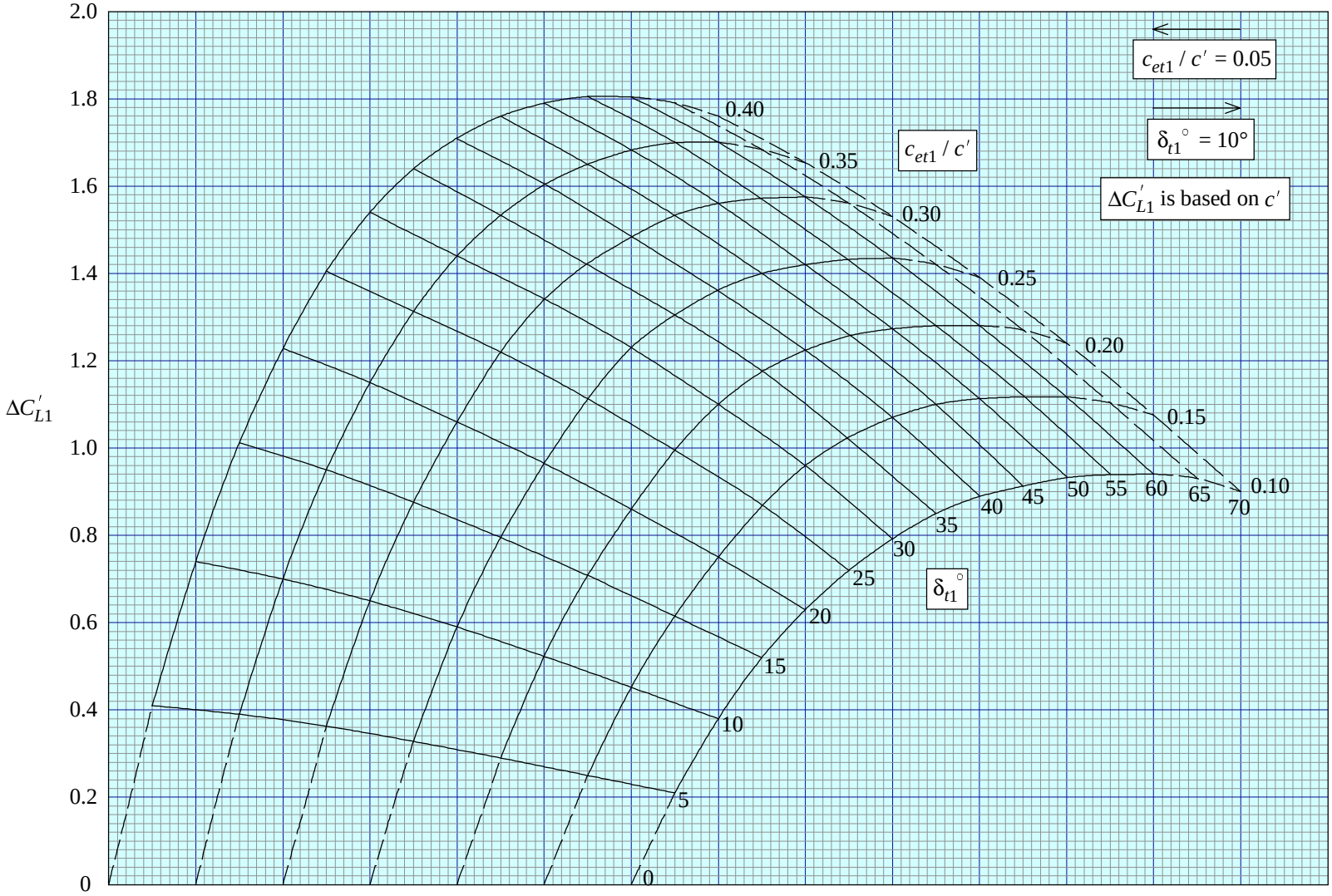

FIGURE 4 LIFT COEFFICIENT INCREMENT ASSOCIATED WITH DEPLOYMENT OF FIRST ELEMENT OF SLOTTED FLAP ON AEROFOIL

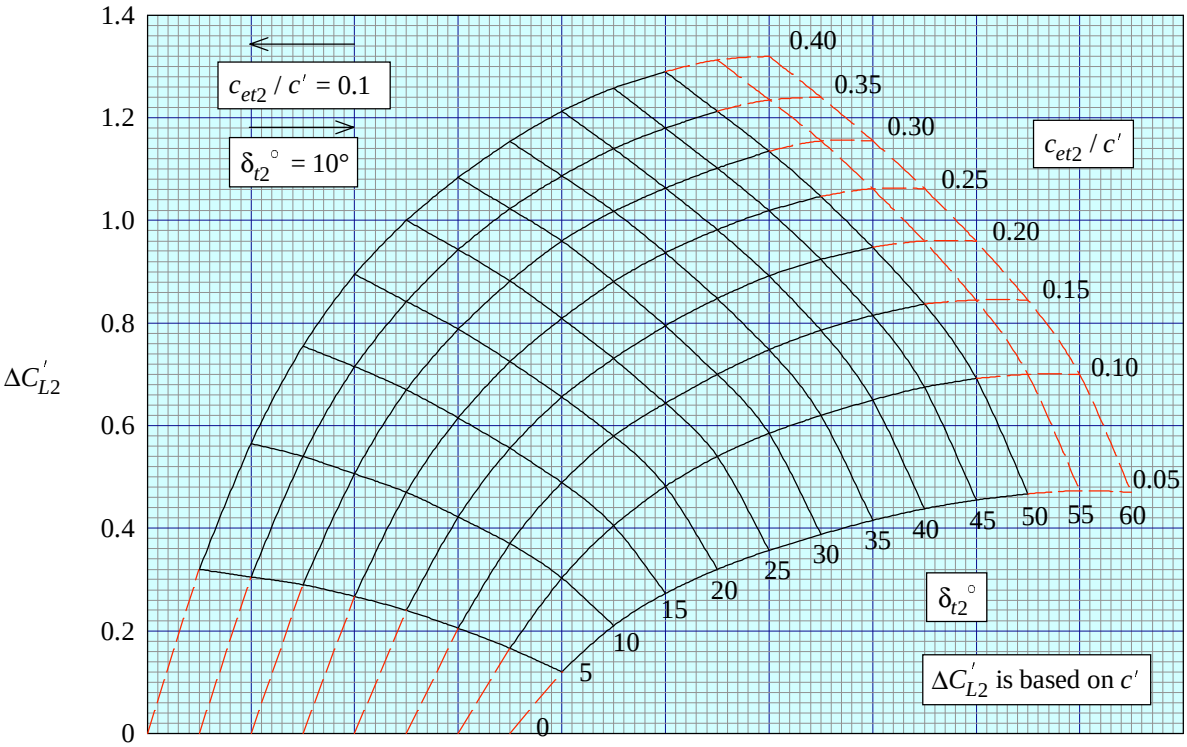

FIGURE 5 LIFT COEFFICIENT INCREMENT ASSOCIATED WITH DEPLOYMENT OF SECOND ELEMENT OF SLOTTED FLAP ON AEROFOIL

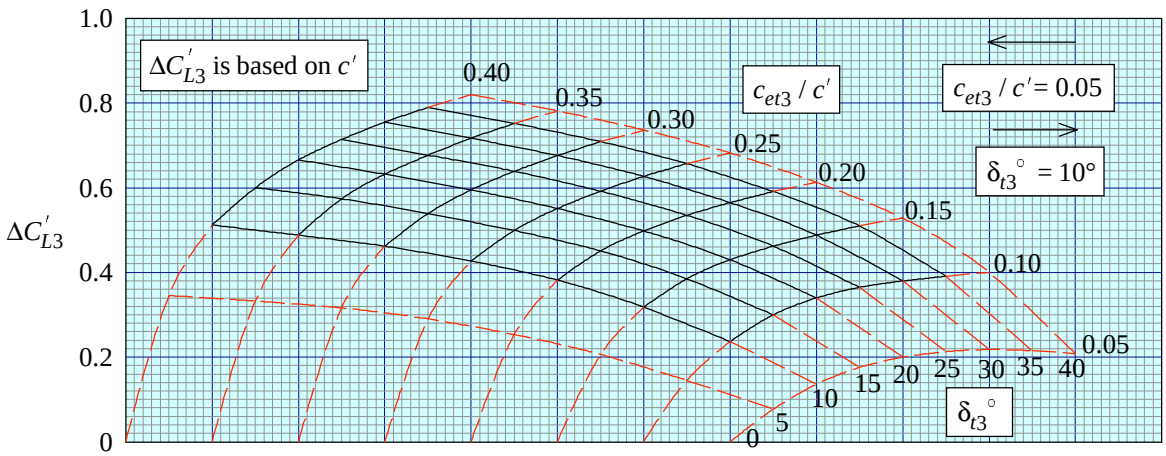

FIGURE 6 LIFT COEFFICIENT INCREMENT ASSOCIATED WITH DEPLOYMENT OF THIRD ELEMENT OF SLOTTED FLAP ON AEROFOIL

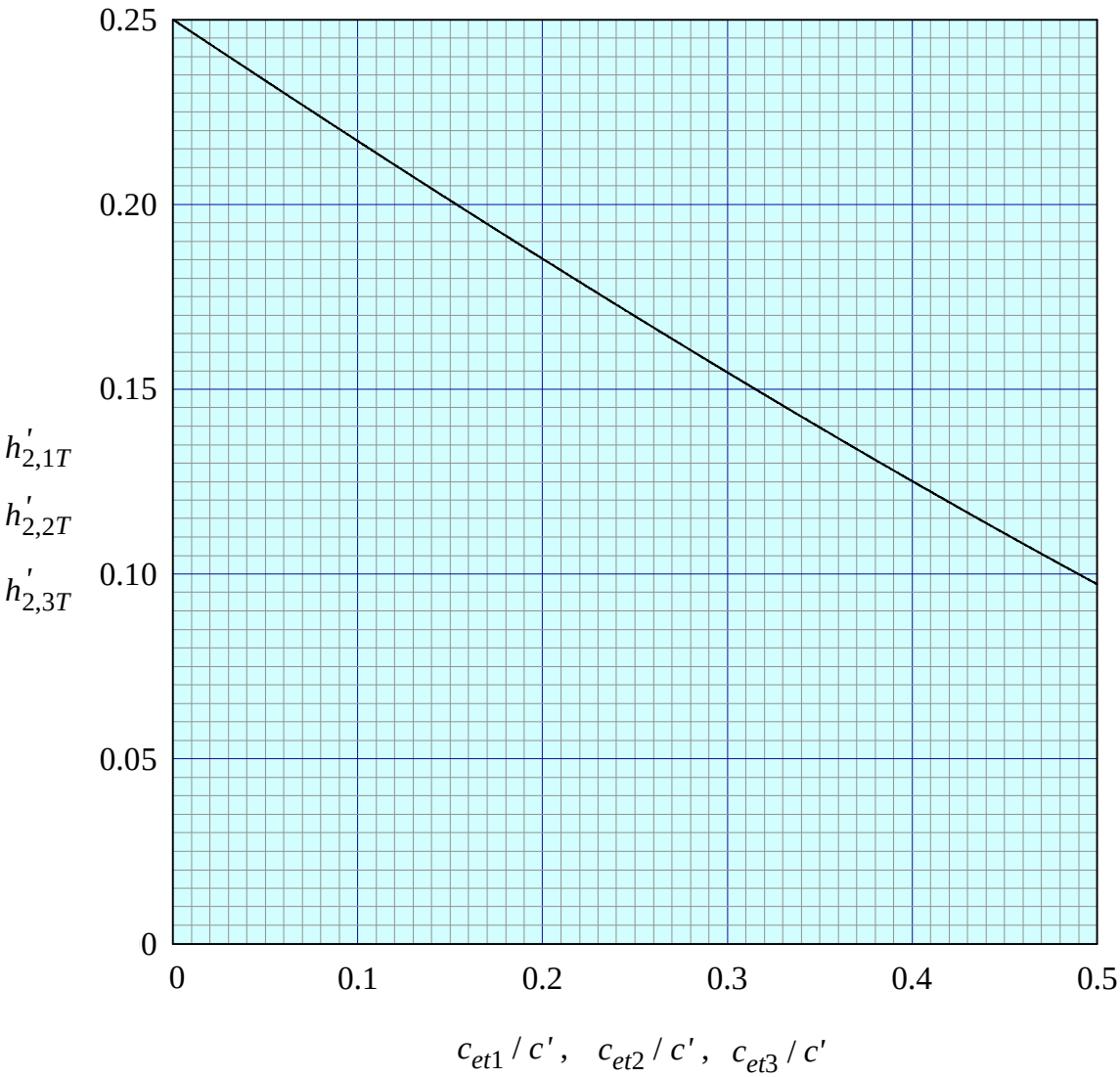

FIGURE 7 THEORETICAL VALUE OF CENTRE OF INCREMENTAL LIFT ON AEROFOIL DUE TO FLAP DEPLOYMENT

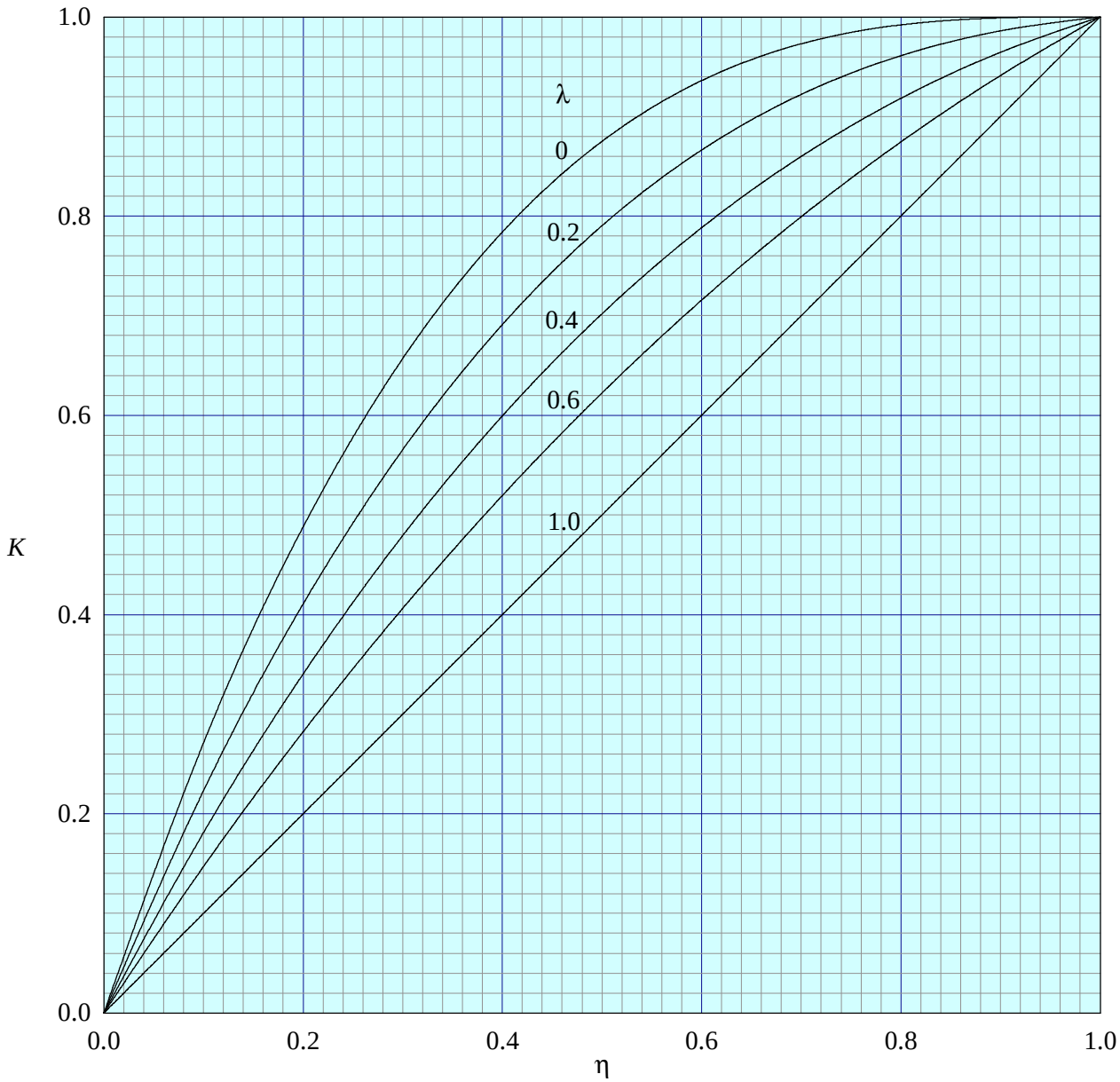

FIGURE 8 PART-SPAN FACTOR *K* FOR DOUBLE-SLOTTED AND TRIPLE-SLOTTED FLAPS

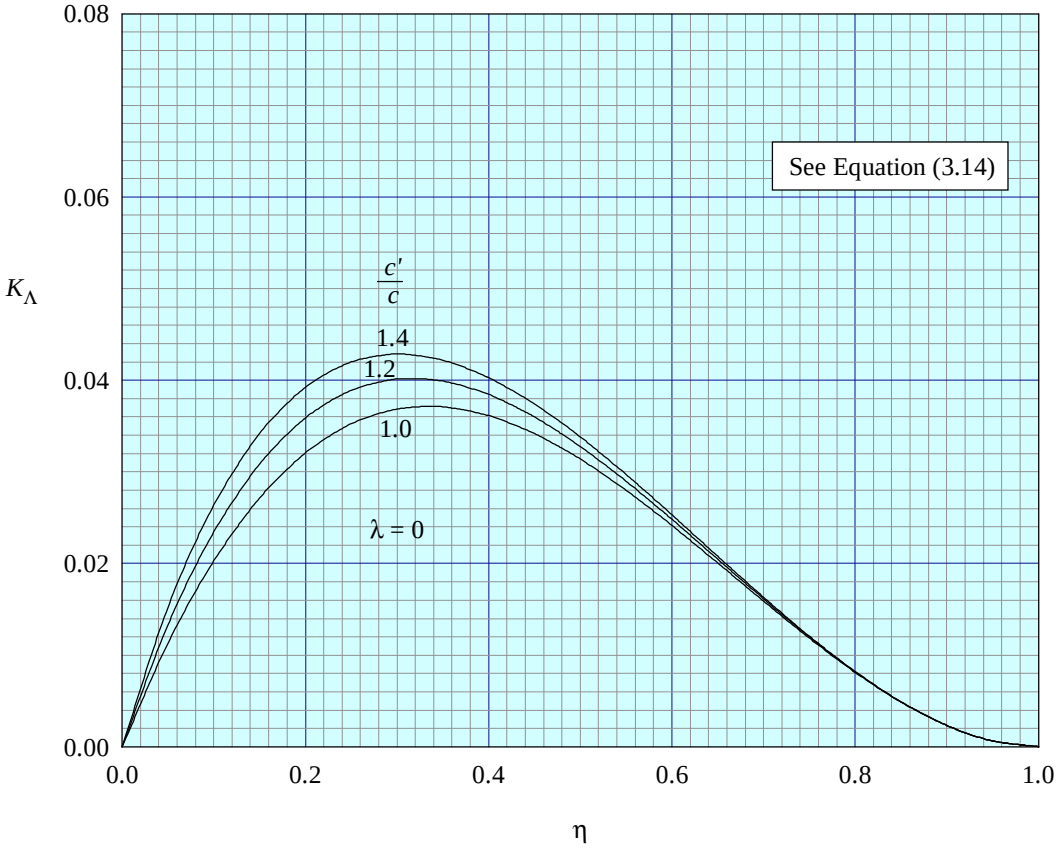

FIGURE 9a PART-SPAN FACTOR K_Λ FOR DOUBLE-SLOTTED AND TRIPLE-SLOTTED FLAPS

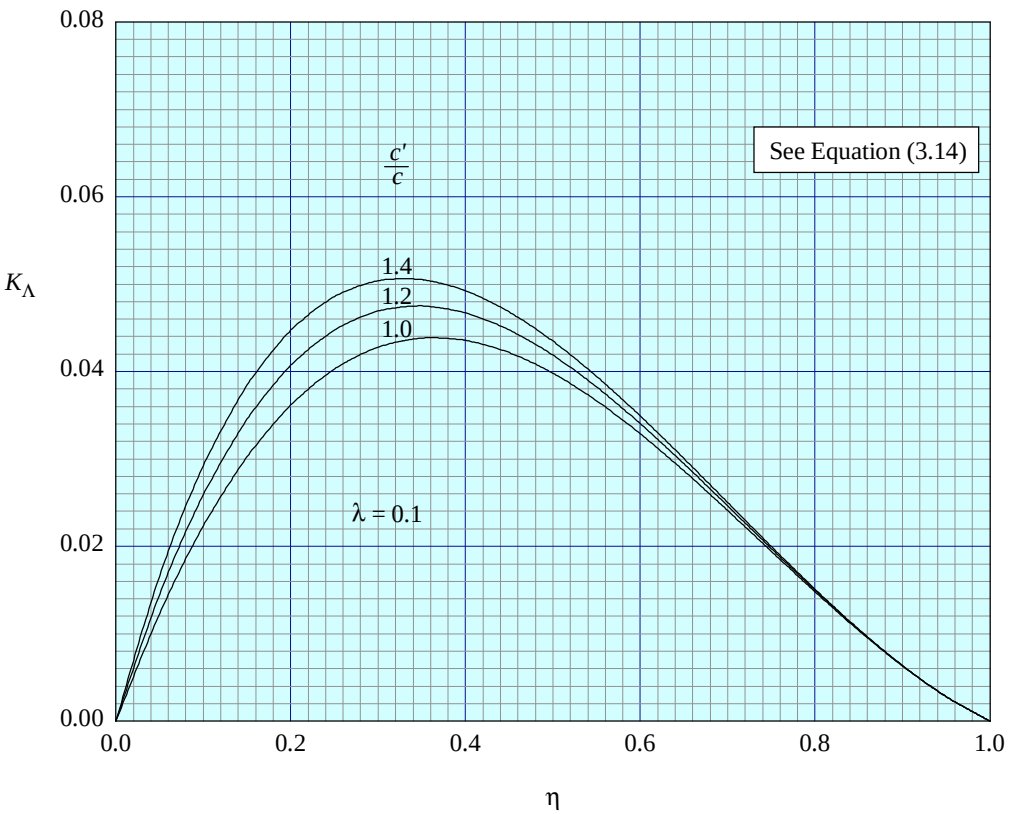

FIGURE 9b PART-SPAN FACTOR K_Λ FOR DOUBLE-SLOTTED AND TRIPLE-SLOTTED FLAPS

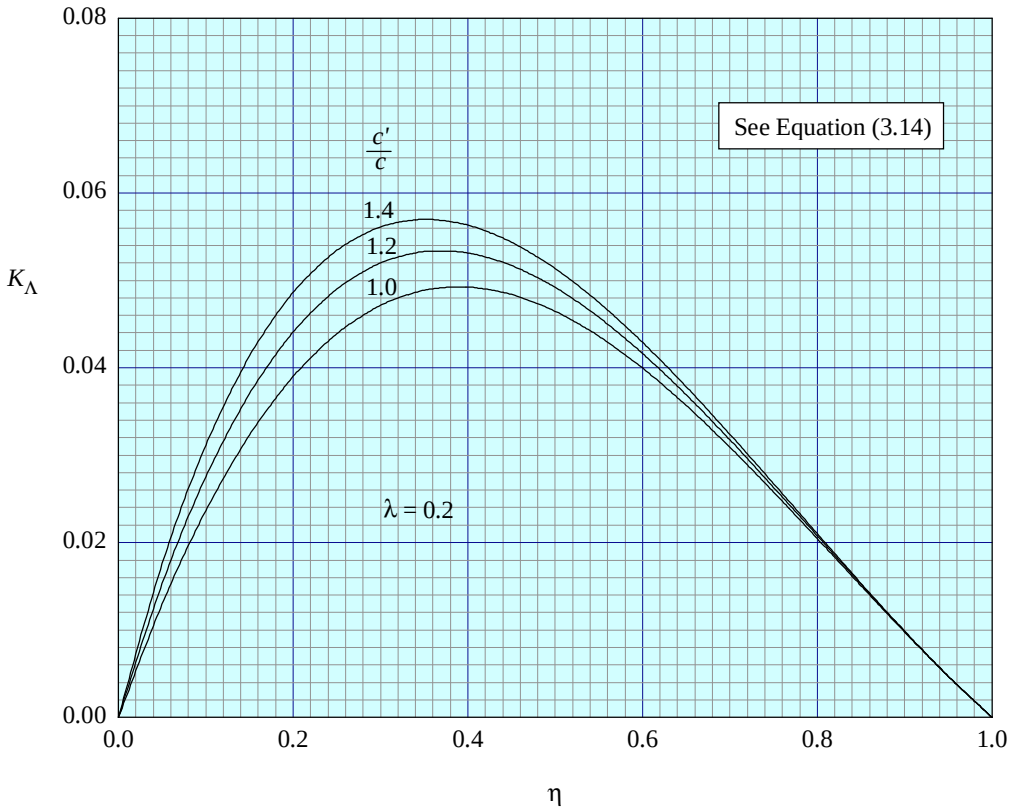

FIGURE 9c PART-SPAN FACTOR K_Λ FOR DOUBLE-SLOTTED AND TRIPLE-SLOTTED FLAPS

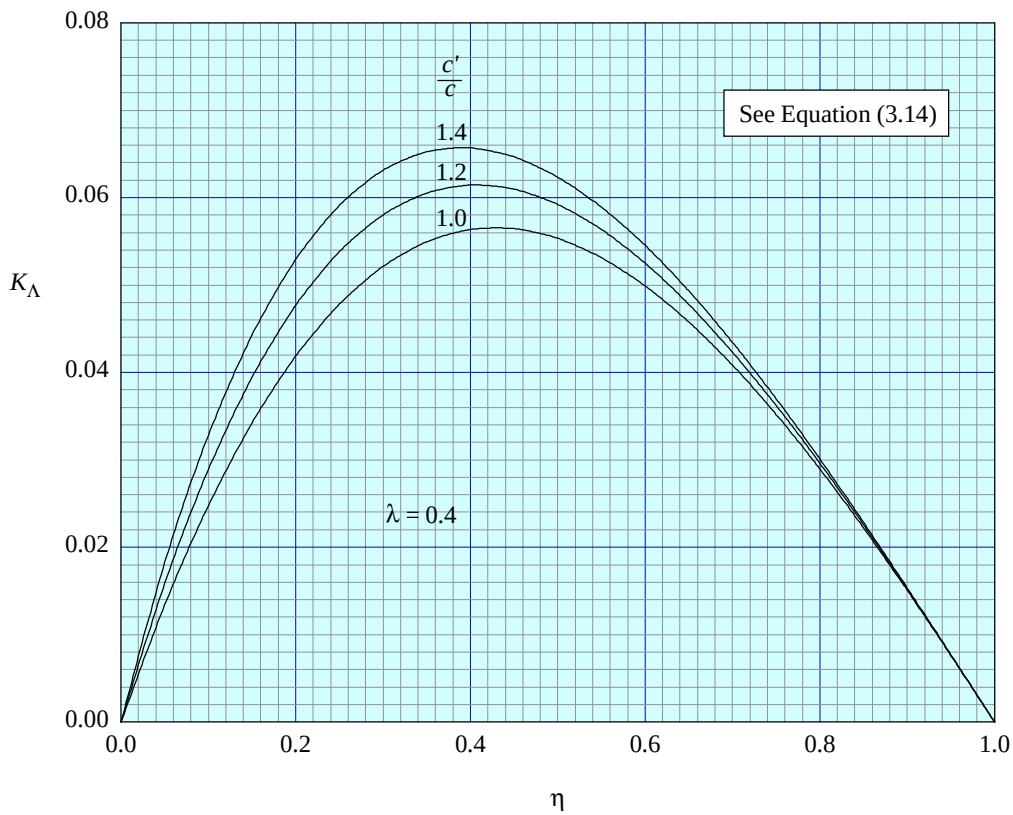

FIGURE 9d PART-SPAN FACTOR K_Λ FOR DOUBLE-SLOTTED AND TRIPLE-SLOTTED FLAPS

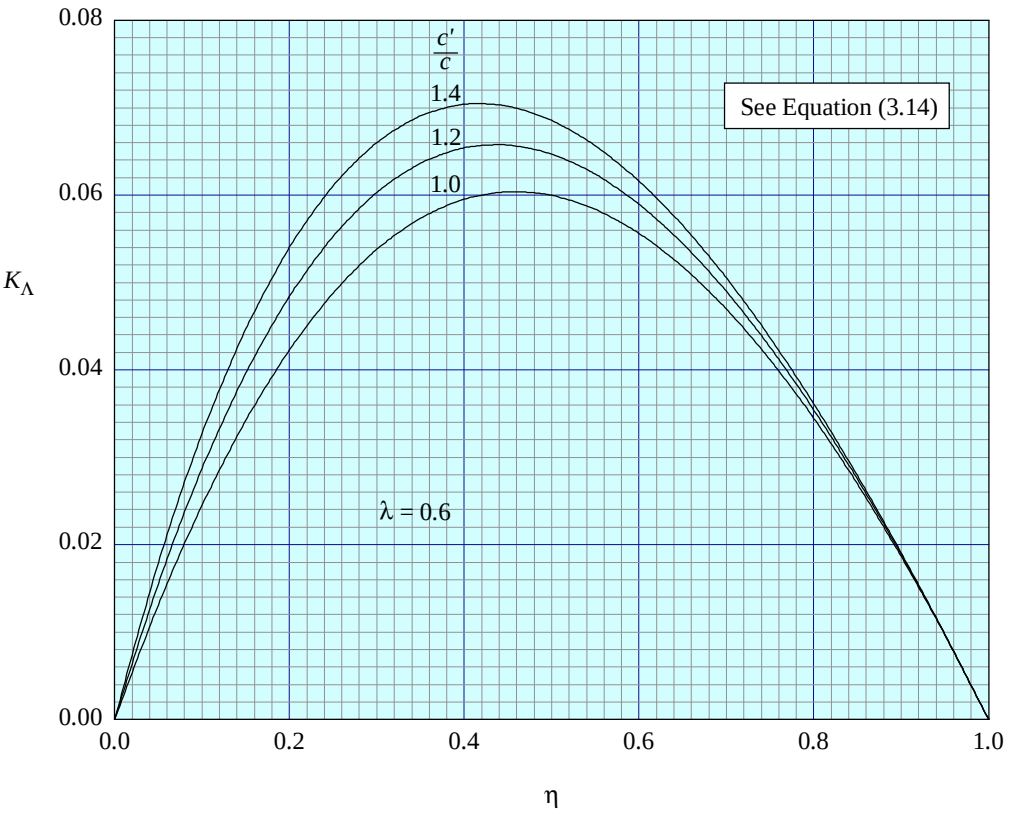

FIGURE 9e PART-SPAN FACTOR K_Λ FOR DOUBLE-SLOTTED AND TRIPLE-SLOTTED FLAPS

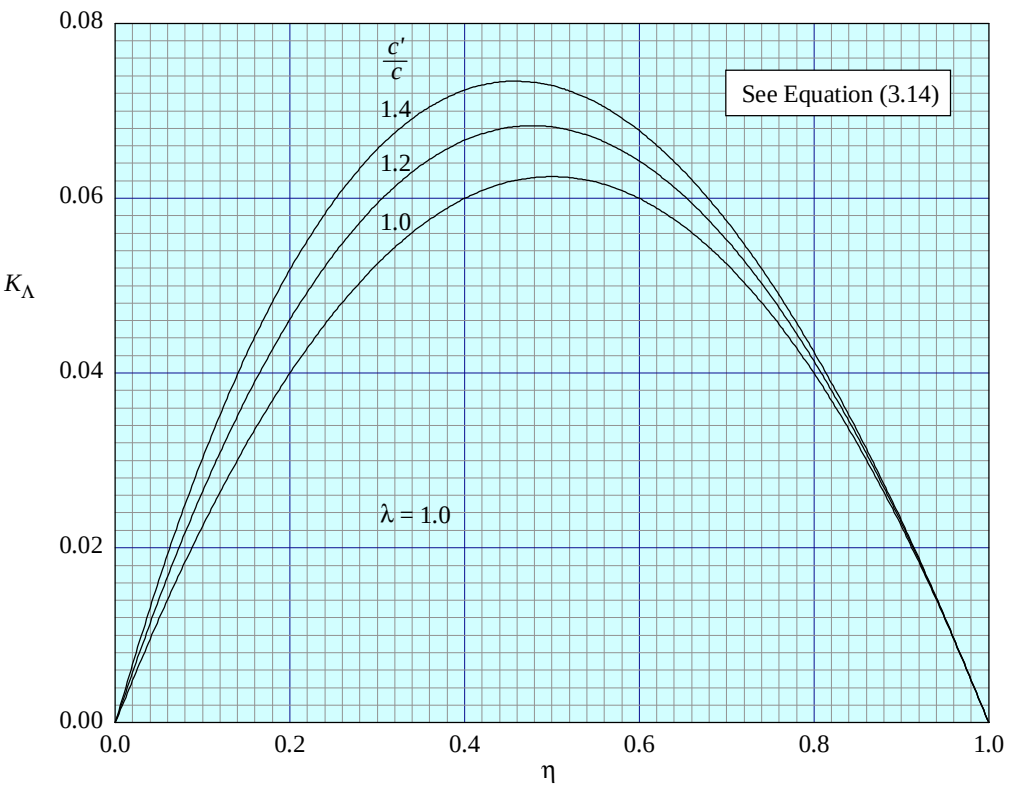

FIGURE 9f PART-SPAN FACTOR K_Λ FOR DOUBLE-SLOTTED AND TRIPLE-SLOTTED FLAPS

ESDU DATA ITEMS

ESDU Data Items provide validated information in engineering design and analysis for use by, or under the supervision of, qualified engineers. The data are founded on an evaluation of all the relevant information, both published and unpublished, and are invariably supported by original work of ESDU staff engineers or consultants. The whole process is subject to independent review for which crucial support is provided by industrial companies, government research laboratories, universities and others from around the world through the participation of some of their leading experts on ESDU Technical Committees. This process ensures that the results of much valuable work (theoretical, experimental and operational), which may not be widely available or in a readily usable form, can be communicated concisely and accurately to the engineering community.

We are constantly striving to develop new work and review data already issued. Any comments arising out of your use of our data, or any suggestions for new topics or information that might lead to improvements, will help us to provide a better service.

THE PREPARATION OF THIS DATA ITEM

The work on this particular Data Item which supersedes, in part, Item Nos Aero F.08.01.01 and 02 was monitored and guided by the Aerodynamics Committee which first met in 1942 and now has the following membership:

Chairman

Mr H.C. Garner	—	Independent

Members

Dr M.Z. Bouter*	—	Raytheon Aircraft Co., Wichita, Kansas, USA
Mr P.D. Chappell	—	Independent
Dr P.C. Dexter	—	British Aerospace plc, Sowerby Research Centre, Bristol
Mr J.R.J. Dovey	—	Independent
Dr K.P. Garry	—	Cranfield University
Mr D.H. Graham*	—	Northrop Grumman Corp., Pico Rivera, Calif., USA
Mr M.J. Green	—	Independent
Dr H.P. Horton	—	Queen Mary and Westfield College, University of London
Dr D.W. Hurst	—	University of Glasgow
Mr M. Jager*	—	Boeing, Long Beach, Calif., USA
Mr K. Karling*	—	Saab-Scania AB, Linköping, Sweden
Dr E.H. Kitchen	—	Rolls Royce plc, Derby
Miss M. Maina	—	Aircraft Research Association
Mr M. Maurel	—	Aérospatiale, Toulouse, France
Mr C.M. Newbold	—	DERA, Farnborough
Mr J.B. Newton	—	British Aerospace Defence Ltd, Warton
Mr M.J. Pow	—	British Aerospace Airbus Ltd, Filton
Mr R. Sanderson	—	Daimler-Benz Aerospace Airbus, GmbH, Bremen, Germany
Mr J. Tweedie	—	Short Brothers plc, Belfast
Mr A.J. Wells	—	British Aerospace Regional Aircraft, Woodford

* Corresponding Member.

The technical work involved in the assessment of the available information and the development and subsequent construction of the Data Item method was carried out under contract to ESDU by Mr J.R.J. Dovey.

The person with overall responsibility for the work in this subject area is Mr R.W. Gilbey, Head of Aircraft Aerodynamics Group.